

Optimizing Synchronization, Flow, and Robustness in Weighted Complex Networks

G. Korniss, R. Huang, S. Sreenivasan, and B.K. Szymanski

Social and Cognitive Networks Academic Research Center, Rensselaer Polytechnic Institute, 110 8th Street, Troy, NY 12180–3590, USA

Summary. Complex biological, social, and technological systems can be often modeled by weighted networks. The network topology, together with the distribution of available link or node capacity (represented by weights) and subject to cost constraints, strongly affect the dynamics or performance of the networks. Here, we investigate optimization in fundamental synchronization and flow problems where the weights are proportional to $(k_i k_j)^\beta$ with k_i and k_j being the degrees of the nodes connected by the edge. In the context of synchronization, these weights represent the allocation of limited resources (coupling strength), while in the associated random walk and current flow problems, they control the extent of hub avoidance, relevant in routing and search. In this Chapter, we review fundamental connections between stochastic synchronization, random walks, and current flow, and we discuss optimization problems for these processes in the above weighted networks.

1 Introduction

Synchronization [1–6] and transport [7–11] phenomena are pervasive in natural and engineered complex interconnected systems with applications ranging from neurobiology and population dynamics to social, communication, and information networks. In the recent wave of research on complex networks [12–18], the focus has shifted from structure to various dynamical and stochastic processes on networks [19, 20], synchronization and transport are being one of them. The common question addressed by most studies within their specific context is how the collective response of locally-coupled entities is influenced by the underlying network topology.

Here, by network synchronization, we refer to the generic problem where individuals or agents attempt to locally coordinate their actions with their network neighbors or within some spatial neighborhood, in an attempt to improve global performance or reach global agreement [6, 21]. In the broader context, these problems are also referred to as consensus problems [6, 22, 23]. In this Chapter, we will use the terms synchronization and coordination synonymously. Classic examples for coordination phenomena are animal flocking [24–26] and cooperative control of vehicle formation [27], where individual animals or units are adjusting their position, speed, and headings (the relevant local state variables) based on the state of their neighborhood, potentially leading to tight formations. Fundamental synchronization problems have also numerous applications to neurobiology [28–32], population dynamics [33, 34], and load balancing and task allocation problems in distributed computing [21, 35–39].

Research on flow optimization in networks has been around since at least the first data sets on transportation networks became available (for a brief historical review, see Refs. [11, 40]). Perhaps, among the first ones was a study on transportation planning on the Soviet railway network, as early as in 1930 [41], followed by others in the 1940s [42–44]. Flow optimization and network interdiction problems also attracted significant interest during the Cold War years [45, 46] and have been a main thrust in operations research since [7, 47, 48].

The increasing availability of data on real-life complex biological, information, social, and infrastructure networks, and the emerging novel type of network structures have triggered a recent wave on fundamental research on transport and flow in networks [49–83]. Connections between random walks and resistor networks have been discussed in detail in several works [84–86]. Furthermore, we have recently explored fundamental connections and relations (governed by the same underlying network Laplacian) between stochastic synchronization problems and resistor networks, current flow, and random walks [10, 87]. In this Chapter, in parallel with reviewing synchronization phenomena in noisy environments, we will discuss some natural and fundamental connections with idealized transport and flow problems on complex networks, in particular, connections with some simplified local and global routing and search schemes [67, 68, 72].

The ultimate challenge in network optimization (of synchronization and flow) is when both the network structure and the link qualities (represented by weighted links) can change or evolve [8, 67], subject to cost constraints. Here, we review and discuss a simpler set of problems, where the network structure is fixed but the link weights (or coupling strengths) can be allocated. In particular, we consider a specific and symmetric form of the weights on uncorrelated scale-free (SF) networks, being proportional to $(k_i k_j)^\beta$ where k_i and k_j are the degrees of the nodes connected by the link [10, 88–91]. The above general form has been suggested by empirical studies of metabolic [50] and airline transportation networks [51]. We discuss the effects of such a weighting scheme in our synchronization and flow problems. Then the task becomes maximizing the synchronization efficiency, throughput, or robustness as a function of β .

The setup of this Chapter is as follows. In Sec. 2 we review optimization of synchronization in a noisy environment [10]. In Sec. 3 and 4, we present results for optimization of resistor networks and random walks, respectively, together with reviewing fundamental connections between the relevant observables in synchronization, resistor networks, and random walks. In Sec. 5 we discuss current-flow betweenness and optimization of throughput in weighted complex networks [92]. In Sec. 6 we present results on shortest-path betweenness, cascading failures, and cascade control in weighted complex networks.

2 Synchronization in a Noisy Environment in Weighted Networks

A large number of studies investigated the Kuramoto model of coupled oscillators [4, 93], naturally generalized to complex networks [94–96]. The common feature of the findings is the spontaneous emergence of order (synchronous phase) on complex networks, qualitatively similar to that observed on fully-connected networks (also referred to as complete graphs), in contrast to regular networks in low dimensions. Another large group of studies addressed synchronization in coupled nonlinear dynamical systems (e.g., chaotic oscillators) [3] on small-world (SW) [97] and scale-free (SF) [88, 98–101] networks. The analysis of synchronization in the latter models can be carried out by linearization about the synchronous state and using the framework of the master stability function [102]. In turn, the technical challenge of the problem is reduced to the diagonalization of the Laplacian on the respective network, and

calculating or estimating the eigenratio [97] (the ratio of the largest and the smallest non-zero eigenvalue of the network Laplacian), a characteristic measure of synchronizability (smaller eigenratios imply better synchronizability). Along these lines, a number of recent studies considered not only complex, possibly heterogeneous, interaction topologies between the nodes, but also weighted (heterogeneities in the strength of the couplings) [49, 88, 99, 100] and directed networks [103–105].

In a more general setting of synchronization problems, the collective behavior/response of the system is obviously strongly influenced by the nonlinearities, the coupling/interaction topology, the weights/strength of the (possibly directed) links, and the presence and the type of noise [3, 101]. Here, we study synchronization in weighted complex networks with linear coupling in the presence of delta-correlated white noise. Despite its simple formulation, this problem captures the essential features of fundamental stochastic synchronization, consensus, and coordination problems with application ranging from coordination and load balancing causally-constrained queuing networks [106, 107] to e-commerce-based services facilitated by interconnected servers [108], and certain distributed-computing schemes on computer networks [21, 36–39]. This simplified problem is the Edwards-Wilkinson (EW) process [109] on the respective network [10, 87, 110–115], and is described by the Langevin equation

$$\partial_t h_i = - \sum_{j=1}^N C_{ij}(h_i - h_j) + \eta_i(t), \quad (1)$$

where $h_i(t)$ is the general stochastic field variable on a node (such as fluctuations in the task-completion landscape in certain distributed parallel schemes on computer networks [21, 111, 112]) and $\eta_i(t)$ is a delta-correlated noise with zero mean and variance $\langle \eta_i(t) \eta_j(t') \rangle = 2\delta_{ij} \delta(t - t')$. Here, $C_{ij} = C_{ji} > 0$ is the symmetric coupling strength between the nodes i and j ($C_{ii} = 0$). Note that without the noise term, the above equation is also referred to as the consensus problem [6, 22, 23] on the respective network (in the sense of networked agents trying to reach an agreement, balance, or coordination regarding a certain quantity of interest). Defining the network Laplacian,

$$\Gamma_{ij} \equiv \delta_{ij} C_i - C_{ij}, \quad (2)$$

where $C_i \equiv \sum_l C_{il}$, we can rewrite Eq. (1)

$$\partial_t h_i = - \sum_{j=1}^N \Gamma_{ij} h_j + \eta_i(t). \quad (3)$$

For the steady-state equal-time two-point correlation function one finds

$$G_{ij} \equiv \langle (h_i - \bar{h})(h_j - \bar{h}) \rangle = \hat{\Gamma}_{ij}^{-1} = \sum_{k=1}^{N-1} \frac{1}{\lambda_k} \psi_{ki} \psi_{kj}, \quad (4)$$

where $\bar{h} = (1/N) \sum_{i=1}^N h_i$ and $\langle \dots \rangle$ denotes an ensemble average over the noise in Eq. (3). Here, $\hat{\Gamma}^{-1}$ denotes the inverse of Γ in the space orthogonal to the zero mode. Also, $\{\psi_{ki}\}_{i=1}^N$ and λ_k , $k = 0, 1, \dots, N-1$, denote the k th normalized eigenvectors and the corresponding eigenvalues, respectively. The $k = 0$ index is reserved for the zero mode of the Laplacian on the network: all components of this eigenvector are identical and $\lambda_0 = 0$. The last form in Eq. (4) (the spectral decomposition of $\hat{\Gamma}^{-1}$) can be used to directly employ the results of exact numerical diagonalization.

For the EW process on any network, the natural observable is the steady-state width or spread of the synchronization landscape [87, 111, 112, 115–117]

$$\langle w^2 \rangle \equiv \left\langle \frac{1}{N} \sum_{i=1}^N (h_i - \bar{h})^2 \right\rangle = \frac{1}{N} \sum_{i=1}^N G_{ii} = \frac{1}{N} \sum_{k=1}^{N-1} \frac{1}{\lambda_k}. \quad (5)$$

The above observable is typically self-averaging (confirmed by numerics), i.e., the width $\langle w^2 \rangle$ for a sufficiently large, single network realization approaches the width averaged over the network ensemble. A network is said to be synchronizable if the width has a finite steady-state value; the smaller the width, the better the synchronization. Finite and connected (single component) networks are always synchronizable. In the limit of infinite network size, however, network ensembles with a vanishing (Laplacian) spectral gap may become unsynchronizable, depending on the details of the small- λ behavior of the density of eigenvalues [5, 21].

The focus of this section is to optimize synchronization (i.e., minimize the width) on (i) weighted uncorrelated networks with SF degree distribution, (ii) subject to a fixed cost. In the context of this work, we define the total cost C_{tot} simply to equal to the sum of weights over all edges in the network

$$\sum_{i<j} C_{ij} = \frac{1}{2} \sum_{i,j} C_{ij} = C_{tot}. \quad (6)$$

The elements of the coupling matrix C_{ij} can be expressed in terms of the network's adjacency matrix A_{ij} and the assigned weights W_{ij} connecting node i and j as $C_{ij} = W_{ij}A_{ij}$. Here, we consider networks where the weights are symmetric and proportional to a power of the degrees of the two nodes connected by the link, $W_{ij} \propto (k_i k_j)^\beta$. We choose our cost constraint to be such that it is equal to that of the unweighted network, where each link is of unit strength.

$$\sum_{i,j} C_{ij} = 2C_{tot} = \sum_{i,j} A_{ij} = N\bar{k}, \quad (7)$$

where $\bar{k} = \sum_i k_i / N = \sum_{i,j} A_{ij} / N$ is the mean degree of the graph, i.e., the average cost per edge is fixed. Thus, the question we ask, is how to allocate the strength of the links in networks with heterogeneous degree distributions with a fixed total cost in order to optimize synchronization. That is, the task is to determine the value of β which minimizes the width Eq. (5), subject to the constraint Eq. (7).

Combining the form of the weights, $W_{ij} \propto (k_i k_j)^\beta$, and the constraint Eq. (7) one can immediately write for the coupling strength between nodes i and j

$$C_{ij} = N\bar{k} \frac{A_{ij}(k_i k_j)^\beta}{\sum_{l,n} A_{ln}(k_l k_n)^\beta} \quad (8)$$

From the above it is clear that the distribution of the weights is controlled by a single parameter β , while the total cost is fixed, $C_{tot} = N\bar{k}/2$.

Before tackling the above optimization problem for the restricted set of heterogeneous networks and the specific form of weights, it is useful to determine the minimum attainable value of the width of the EW synchronization problem in any network with symmetric couplings. This value will serve as a ‘‘baseline’’ reference for our problem. In Appendix 1 we show that this absolute minimum value of the width is

$$\langle w^2 \rangle_{\min} = \frac{(N-1)^2}{2NC_{tot}} \quad (9)$$

and can be realized by the fully connected network.

If one now considers the synchronization problem on any network with N nodes, with average degree \bar{k} and with total cost $C_{tot} = N\bar{k}/2$ to be optimized in some fashion [e.g., with

respect to a single parameter β , Eq. (8)], the above result provides an absolute lower bound for the optimal width

$$\langle w^2(\beta) \rangle_{\min} \geq \frac{(N-1)^2}{N^2} \frac{1}{\bar{k}} \simeq \frac{1}{\bar{k}}. \quad (10)$$

2.1 Mean-field approximation on uncorrelated SF networks

First, we approximate the equations of motion [Eq. (1)] by replacing the local weighted average field $(1/C_i) \sum_j C_{ij} h_j$ with the global average \bar{h} (the mean-height)

$$\begin{aligned} \partial_t h_i &= - \sum_{j=1}^N C_{ij} (h_i - h_j) + \eta_i(t) = -C_i \left(h_i - \frac{\sum_j C_{ij} h_j}{C_i} \right) + \eta_i(t) \\ &\approx -C_i (h_i - \bar{h}) + \eta_i(t). \end{aligned} \quad (11)$$

Note that $C_i \equiv \sum_j C_{ij}$ is the weighted degree. As can be directly seen by summing up Eq. (1) over all nodes, the mean height \bar{h} performs a simple random walk with noise intensity $\mathcal{O}(1/N)$. Thus, in the mean-field (MF) approximation (see details in Appendix 2), in the asymptotic large- N limit, fluctuations *about the mean* decouple and reach a stationary distribution with variance

$$\langle (h_i - \bar{h})^2 \rangle \approx 1/C_i, \quad (12)$$

yielding

$$\langle w^2 \rangle = \frac{1}{N} \sum_{i=1}^N \langle (h_i - \bar{h})^2 \rangle \approx \frac{1}{N} \sum_i \frac{1}{C_i}. \quad (13)$$

Now we consider uncorrelated weighted SF networks, with a degree distribution

$$P(k) = (\gamma - 1) m^{\gamma-1} k^{-\gamma}, \quad (14)$$

where m is the minimum degree in the network and $2 < \gamma \leq 3$. The average and the minimum degree are related through $\langle k \rangle = m(\gamma - 1)/(\gamma - 2)$. Using the approximation for the weighted degree $C(k)$ of a node with degree k in uncorrelated (UC) weighted SF graphs (see Appendix 3),

$$C(k) \approx \frac{\gamma - 2 - \beta}{\gamma - 2} \frac{k^{\beta+1}}{m^\beta}, \quad (15)$$

and assuming self-averaging for large enough networks, one obtains for the width of the synchronization landscape

$$\langle w^2(\beta) \rangle \approx \frac{1}{N} \sum_i \frac{1}{C_i} \approx \int_m^\infty dk P(k) \frac{1}{C(k)} = \frac{1}{\langle k \rangle} \frac{(\gamma - 1)^2}{(\gamma - 2 - \beta)(\gamma + \beta)}, \quad (16)$$

where using infinity as the upper limit is justified for $\gamma + \beta > 0$. Elementary analysis yields the main features of the above expression for the average width:

1. $\langle w^2(\beta) \rangle$ is minimum at $\beta = \beta^* = -1$, *independent* of the value of γ .
2. $\langle w^2 \rangle_{\min} = \langle w^2(\beta^*) \rangle = 1/\langle k \rangle$

The above approximate result is consistent with using infinity as the upper limit in all integrals, in that the optimal value $\beta^* = -1$ falls inside the interval $-\gamma < \beta < \gamma - 2$ for $2 < \gamma \leq 3$. Interestingly, one can also observe, that, in this approximation, the minimal value of the width

is equal to that of the global optimum [Eq. (10)], realized by the fully-connected network of the same cost $N\langle k\rangle/2$, i.e. with identical links of strength $\langle k\rangle/(N-1)$.

We emphasize that in obtaining the above result [Eq. (16)] we employed two very strong and distinct assumptions/approximations: (i) for the dynamics on the network, we neglected correlations (in a MF fashion) between the local field variables and approximated the local height fluctuations by Eq. (12); (ii) we assumed that the network has no degree-degree correlations between nodes which are connected (UC), so that the “weighted degree” of a node with degree k , $C(k)$ can be approximated with Eq. (15) for networks with $m\gg 1$.

2.2 Numerical results

For comparison with the above mean-field results, we considered Barabási-Albert (BA) SF networks [13, 14], “grown” to N nodes¹, where $P(k) = 2m^2/k^3$, i.e., $\gamma = 3$. While growing networks, in general, are not uncorrelated, degree-degree correlations are anomalously (marginally) weak for the BA network [18, 118].

We have performed exact numerical diagonalization and employed Eq. (4) to find the local height fluctuations and Eq. (5) to obtain the width for a given network realization. We carried out the above procedure for 10–100 independent network realizations. Finite-size effects (except for the $m=1$ BA tree network) are very weak for $-2 < \beta < 0$; the width essentially becomes independent of the system size in this interval. Figure 1 displays result for the local height fluctuations as a function of the degree of the node. We show both the fluctuations averaged over all nodes with degree k and the scattered data for individual nodes. One can observe that our approximate results for the scaling with the degree [combining Eqs. (12) and (58)], $\langle (h_i - \bar{h})^2 \rangle \approx 1/C_i \sim k_i^{-(\beta+1)}$, work very well, except for very low degrees. The special case $\beta=0$, is exceptionally good, since here $C_i = \sum_j A_{ij} = k_i$ exactly, and the only approximation is Eq. (12).

In Fig. 2, we show our numerical results for the width and compare it with the approximate (MF+UC) results Eq. (16). The divergence of the approximate result Eq. (16) at $\beta = -3$ and $\beta = 1$ is the artifact of using infinity as the upper limit in the integrals performed in our approximations. The results for the width clearly indicate the existence of a minimum at a value of β^* somewhat greater than -1 . Further analysis reveals [10] that as the minimum degree m is increased, the optimal β approaches -1 from above. This is not surprising, since in the limit of $m \gg 1$ (large minimum degree), both the MF and the UC part of our approximations are expected to work progressively better. For $\beta=0$, our approximation [Eq. (16)] is within 8%, 4%, and 1% of the results extracted from exact numerical diagonalization through Eq. (5), for $m=10$, $m=20$, and $m=100$, respectively [10]. For $\beta=-1$, it is within 15%, 7%, and 3% of the numerical results for $m=10$, $m=20$, and $m=100$, respectively [10]. Thus, our approximation works reasonably well for large uncorrelated SF networks with sufficiently large minimum (and consequently, average) degree, i.e., in the $1 \ll m \ll N$ limit. Although for sparse networks with small average degree the MF+UC approximation fails to locate the minimum and the value of the width precisely, nevertheless it provides insight for an efficient optimization of the global performance of weighted heterogeneous networks with a single parameter β , as opposed to a computationally prohibitive exhaustive search. For a detailed quantitative analysis of the error of the MF+UC approximation in the context of the closely related random walks on weighted SF networks (Sec. 4) see Ref. [91].

¹ For the BA scale-free model [13] (growth and preferential attachment), each new node is connected to the network with m links, resulting in $\langle k \rangle \simeq 2m$ in the large- N limit. Here, we employed a fully-connected initial cluster of $m+1$ nodes.

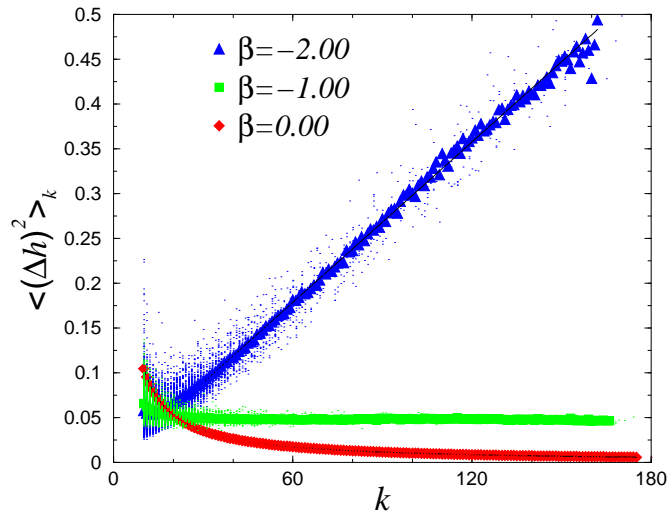


Fig. 1. Height fluctuations as a function of the degree of the nodes for $N=1000$, $\langle k \rangle = 20$, and for $\beta=-2.00$, $\beta=-1.00$, and $\beta=0.00$ (from top to bottom). Data, represented by filled symbols, are averaged over all nodes with degree k . Scatter plot (dots) for individual nodes is also shown from ten network realizations. Solid lines correspond to the MF+UC scaling $\langle (\Delta h)^2 \rangle_k \sim k^{-(\beta+1)}$.

The above optimal link-strength allocation at around the value $\beta^* \approx -1$ seems to be present in all random networks where the degree distribution is different from a delta-function. For example, in SW networks², although the degree distribution has an exponential tail, $\langle w^2 \rangle$ also exhibits a minimum, but the effect is much weaker, as shown in Fig. 2. Further, a point worthwhile to mention, a SW network with the same number of nodes and the same average degree (corresponding to the same cost) always “outperforms” its SF counterpart (in terms of minimizing the width). The difference between their performance is smallest around the optimal value, where both are very close to that of the lowest possible value, realized by the FC network of the same cost.

3 Weighted Resistor Networks

Resistor networks have been widely studied since the 70’s as models for conductivity problems and classical transport in disordered media [121, 122]. Amidst the emerging research on complex networks, resistor networks have been employed to study and explore community structures in social networks [123–126] and centrality measures in information networks [127].

² Here we constructed SW networks by *adding* random links [111, 119, 120] on top of a regular ring with two nearest neighbors. The density of random links per node is p , resulting in an average degree $\langle k \rangle = 2 + p$.

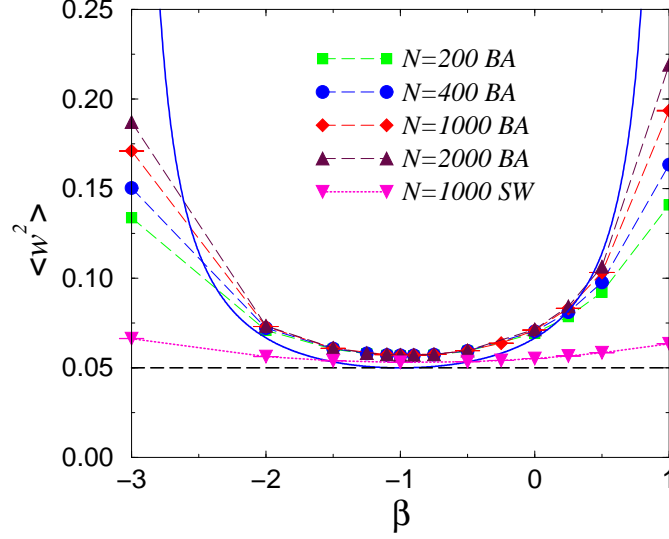


Fig. 2. Steady-state width of the EW synchronization landscape as a function of the weighting parameter β for the BA networks with $m=10$ ($\langle k \rangle \simeq 2m=20$) for various network sizes. The solid curve is the approximate (MF+UC) result [Eq. (16)]. For comparison, numerical results for a SW networks with $N=1000$ and with the same degree is also shown. The horizontal dashed line indicates the absolute lower bound Eq. (10), as achieved by the fully connected network with the same cost $N\langle k \rangle/2$.

Also, electrical networks with directed links (corresponding to diodes) have been used to propose novel page-ranking methods for search engines on the World-Wide-Web [128].

Most recently, simple resistor networks were utilized to study transport efficiency in SF [79,80] and SW networks [87]. The work by López et al. [80] revealed that in SF networks [13, 14] anomalous transport properties can emerge, displayed by the power-law tail of distribution of the network conductance. Now, we consider weighted resistor networks subject to a fixed total cost (the cost of each link is associated with its conductance). As we have shown [10, 87] the relevant observables in the EW synchronization problem and in (Ohmic) resistor networks are inherently related through the spectrum of the network Laplacian. Consider an arbitrary (connected) network where C_{ij} is the conductance of the link between node i and j , with a current I entering (leaving) the network at node s (t). Kirchhoff's and Ohm's laws provide the relationships between the stationary currents and voltages [87, 129]

$$\sum_j C_{ij}(V_i - V_j) = I(\delta_{is} - \delta_{it}), \quad (17)$$

or equivalently,

$$\sum_j \Gamma_{ij} V_j = I(\delta_{is} - \delta_{it}), \quad (18)$$

where Γ_{ij} is the network Laplacian, as defined in the context of the EW process [Eq. (2)]. Introducing the voltages measured from the mean at each node, $\hat{V}_i = V_i - \bar{V}$, where $\bar{V} = (1/N) \sum_{i=1}^N V_i$, one obtains [87]

$$\hat{V}_i = I(G_{is} - G_{it}). \quad (19)$$

Here, G is the same network propagator discussed in the context of the EW process, i.e. the inverse [Eq. (4)] of the network Laplacian [Eq. (2)] in the space orthogonal to the zero mode. Applying Eq. (19) to nodes s and t , where the voltage drop between these nodes is $V_{st} = \hat{V}_s - \hat{V}_t$, one immediately obtains the effective two-point resistance of the network between nodes s and t [87, 129],

$$R_{st} \equiv \frac{V_{st}}{I} = G_{ss} + G_{tt} - 2G_{st} = \sum_{k=1}^{N-1} \frac{1}{\lambda_k} (\psi_{ks}^2 + \psi_{kt}^2 - 2\psi_{ks}\psi_{kt}). \quad (20)$$

The spectral decomposition in Eq. (20) is, again, useful to employ the results of exact numerical diagonalization. Comparing Eqs. (4) and (20), one can see that the two-point resistance of a network between node s and t is the same as the steady-state *height-difference* correlation function of the EW process on the network [87],

$$\langle (h_s - h_t)^2 \rangle = \langle [(h_s - \bar{h}) - (h_t - \bar{h})]^2 \rangle = G_{ss} + G_{tt} - 2G_{st} = R_{st}. \quad (21)$$

For example, using the above relationship and then employing the MF+UC approximation³ one can immediately obtain the scaling of the typical value of the effective two-point resistance in weighted resistance networks, between two nodes with degrees k_s and k_t ,

$$R_{st} \simeq G_{ss} + G_{tt} \sim [k_s^{-(1+\beta)} + k_t^{-(1+\beta)}] = \frac{k_s^{1+\beta} + k_t^{1+\beta}}{(k_s k_t)^{1+\beta}}. \quad (22)$$

A global observable, measuring transport efficiency, analogous to the width of the synchronization landscape, is the average two-point resistance [80, 87] (averaged over all pairs of nodes, for a given network realization). Using Eq. (21) and exploiting the basic properties of the Green's function, one finds

$$\bar{R} \equiv \frac{2}{N(N-1)} \sum_{s<t} R_{st} = \frac{1}{N(N-1)} \sum_{s \neq t} R_{st} = \frac{N}{N-1} 2\langle w^2 \rangle \simeq 2\langle w^2 \rangle, \quad (23)$$

i.e., in the asymptotic large system-size limit the average system resistance of a given network is twice the steady-state width of the EW process on the same network. Note that the above relationships, Eqs. (21) and (23), are exact and valid for any graph.

The corresponding optimization problem for resistor networks then reads as follows: For a fixed total cost, $C_{\text{tot}} = \sum_{i<j} C_{ij} = N\langle k \rangle / 2$, where the link conductances are weighted according to Eq. (8), what is the value of β which minimizes the average system resistance $\bar{R}(\beta)$? Based on the above relationship between the average system resistance and the steady-state width of the EW process on the same graph [Eq. (23)], the answer is the same as was discussed in Sec. 2 [Eq. (16)]: $\beta^* = -1$ and $\bar{R}_{\text{min}} = 2N / [(N-1)\langle k \rangle] \simeq 2/\langle k \rangle$ in the mean-field approximation on uncorrelated random SF networks. Numerical results for $\bar{R}(\beta)$ are also provided for “free” as $\bar{R}(\beta) \simeq 2\langle w^2(\beta) \rangle$, by virtue of the connection Eq. (23) [Fig. 2].

³ In the context of resistor networks, while there are no “fields”, we carry over the terminology “mean-field” (MF) from the associated EW synchronization problem. In terms of the network propagator, the assumptions of the MF approximation can be summarized as $G_{st} \ll G_{ss}$ for all $s \neq t$, and $G_{ss} \simeq 1/C_s$.

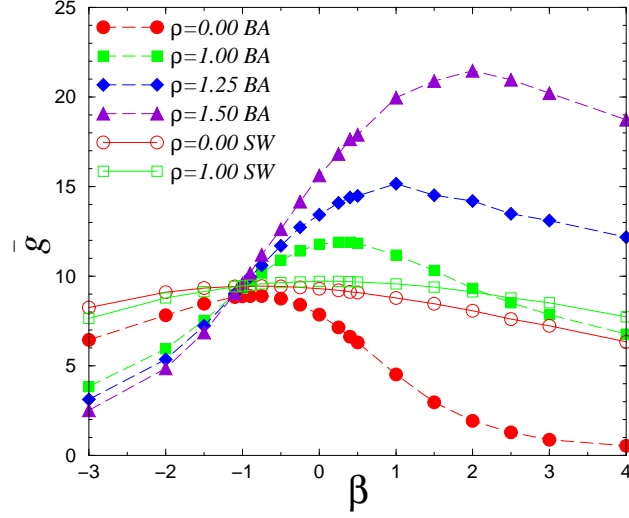


Fig. 3. System conductance vs the edge weight parameter β for different source/target distributions controlled by ρ for BA networks with $m=10$ ($\langle k \rangle \approx 2m=20$) and $N=400$ (solid symbols). For comparison, numerical results for a SW networks with the same network size and average degree is also shown for two ρ values (open symbols).

3.1 Transport optimization for heterogeneous source/target frequencies

As suggested by Lopez et al. [80], the effective (electrical) conductance provides a powerful measure to characterize transport in complex networks. This observable, strongly influenced by the number of disjoint (and possibly weighted) paths between a source and a target, is also closely related to the max-flow problem in networks [7, 11, 40, 63, 81]. The effective two-point conductance is the inverse of the effective two point resistance [Eq. (20)], $g_{st}=1/R_{st}$. If each node is equally likely to be a target or a source, a simple average over all source and target pairs provides the average system conductance, $\bar{g} = \sum_{s \neq t} g_{st} / N(N-1)$. In real systems, however, nodes are not created equal; their relative frequency to be a source or target can greatly vary. In the simplest phenomenological model, we assume that nodes are sources or targets with a frequency proportional k_i^ρ ($\rho \geq 0$) [65, 80]. Also, as previously, we allow the edges (conductivities) to be weighted, controlled by the parameter β according to Eq. (8), subject to a fixed total edge cost Eq. (7). Then, naturally, the relevant global measure is the appropriately weighted system conductance

$$\bar{g}(\beta) = \frac{\sum_{s \neq t} (k_s k_t)^\rho g_{st}(\beta)}{\sum_{s \neq t} (k_s k_t)^\rho}. \quad (24)$$

Then, we consider *optimizing the allocation limited resources* in the above simplified transport problem. That is, for a given source/target distribution controlled by ρ , what is the value of β which minimizes the system conductance $\bar{g}(\beta)$?

In Fig. 3 we show numerical results for BA scale-free networks. When the source/target profile is uniform ($\rho=0$), the system conductance exhibits a maximum at around $\beta \approx -1$ (in

synch with the system resistance exhibiting a minimum around the same β , Fig. 2). For increasing positive values of ρ , the optimal value of β shifts to the right; the location of the maximum of the $\bar{g}(\beta)$ curve for a given ρ quantifies the extent to which resources should be allocated around hubs (or away from hubs) for optimal global performance.

Figure 3 also indicates that the conductance curves for all ρ intersect at around $\beta \approx -1$. Indeed, our previous approximation [Eq. (22)] predicts that at this point the effective two-point conductance $g_{st}=1/R_{st}$ becomes independent of the degree of the source and target nodes, hence the system conductance Eq. (24) become ρ -invariant.

In Fig. 3 we also plot the same system conductance cure for SW networks with the same network size and average degree for two values of ρ . For $\rho=0$ (uniform source/target profile), a SW graph (with a close-to-homogeneous degree distribution) outperforms its BA SF counterpart (with heterogeneous degree distribution) of the same cost for every β . For strongly heterogeneous source/target frequencies ($\rho=1$) the performance of a SW network is better for $\beta < -1$ and $\beta > 2$, while the BA SF network performs better in the $-1 < \beta < 2$ interval.

4 Random Walks in Weighted Networks

Investigating random walks (RW) on networks, and resistor networks can provide invaluable insights into fundamental properties and characteristics of transport and flow on networks [10, 54–56, 80, 84, 87, 91, 130, 131]. In these models, with direct application to search, routing, and information retrieval on networks [132, 133], the connection between network structure and function becomes explicit, so one can address the problems of designing network structures to minimize delivery times, or for a fixed structure, allocating resources (queuing capacity) to minimize load and delays [10, 70, 90].

Here, we consider weights $\{C_{ij}\}$ employed in the previous sections and define a discrete-time random walk (RW) with the transition probabilities [84]

$$P_{ij} \equiv \frac{C_{ij}}{C_i} \quad (25)$$

(recall that $C_i = \sum_l C_{il}$ is the weighted degree). P_{ij} is the probability that the walker currently at node i will hop to node j in the next step. Note that because of the construction of the transition probabilities (being a normalized ratio), the issue of cost constraint disappears from the problem. That is, any normalization prefactor associated with the conserved cost [as in Eq. (8)] cancels out, and the only relevant information is $C_{ij} \propto A_{ij}(k_i k_j)^\beta$, yielding

$$P_{ij} = \frac{C_{ij}}{C_i} = \frac{A_{ij}(k_i k_j)^\beta}{\sum_l A_{il}(k_i k_l)^\beta} = \frac{A_{ij} k_j^\beta}{\sum_l A_{il} k_l^\beta}. \quad (26)$$

Then the results are invariant for any normalization/constraint, so for convenience, one can use the normalized form of the C_{ij} coefficients as given in Eq. (8). As is clear from the above RW transition probabilities, the parameter β controls to what extent “hubs” should be avoided.

Having a random walker starting at an arbitrary source node s , tasked to arrive at an arbitrary target node t , the above weighted RW model can be associated with a simple *local* routing or search scheme [67] where packets are independently forwarded to a nearest neighbor, chosen according to the transition probabilities Eq. (26), until the target is reached. These probabilities contain only limited local information, namely the degree of all neighboring nodes. By construction, the associated local (stochastic) routing problem (Sec. III.B.3)

does not concern link strength (bandwidth) limitations but rather the processing/queuing capabilities of the nodes, so the cost constraint, associated with the links, disappears from the problem.

4.1 Node betweenness for weighted RWs

In network-based transport or flow problems, the appropriate betweenness measure is defined to capture the amount of traffic or information passing through a node or a link, i.e., the load of a node or a link [15, 18, 52–54, 126, 134, 135]. Here, our observable of interest is the *node betweenness* B_i for a given routing scheme [67] (here, purely local and characterized by a single parameter β): *the expected number of visits* to node i for a random walker originating at node s (the source) before reaching node t (the target) $E_i^{s,t}$, summed over all source-target pairs. For a general RW, as was shown by Doyle and Snell [84], $E_i^{s,t}$ can be obtained using the framework of the equivalent resistor-network problem (discussed in Sec. 3). More specifically,

$$E_i^{s,t} = C_i(V_i - V_t), \quad (27)$$

while a *unit* current is injected (removed) at the source (target) node. Utilizing again the network propagator and Eq. (19), one obtains

$$E_i^{s,t} = C_i(V_i - V_t) = C_i(\hat{V}_i - \hat{V}_t) = C_i(G_{is} - G_{it} - G_{ts} + G_{tt}). \quad (28)$$

For the node betweenness, one then obtains

$$\begin{aligned} B_i &= \sum_{s \neq t} E_i^{s,t} = \frac{1}{2} \sum_{s \neq t} (E_i^{s,t} + E_i^{t,s}) = \frac{1}{2} \sum_{s \neq t} C_i(G_{ss} + G_{tt} - 2G_{ts}) \\ &= \frac{C_i}{2} \sum_{s \neq t} R_{st} = \frac{C_i}{2} N(N-1) \bar{R}. \end{aligned} \quad (29)$$

Note that the above expression is valid for any graph and for an arbitrary weighted RW defined by the transition probabilities Eq. (25). As can be seen from Eq. (29), the node betweenness is proportional to the product of a local topological measure, the weighted degree C_i , and a global flow measure, the average system resistance \bar{R} . As a specific case, for the unweighted RW ($\beta=0$) $C_i = \sum_l A_{il} = k_i$, thus, the node betweenness is exactly proportional to the degree of the node, $B_i = k_i N(N-1) \bar{R} / 2$.

Using our earlier approximations and results for uncorrelated SF graphs Eq. (58) and (16), and the relationship between the width and the average system resistance Eq. (23), for weighted RW, controlled by the exponent β , we find

$$B_i(\beta) = \frac{C_i}{2} N(N-1) \bar{R} = C_i N^2 \langle w^2 \rangle \approx N^2 \frac{\gamma-1}{\gamma+\beta} \frac{k_i^{1+\beta}}{m^{1+\beta}}. \quad (30)$$

First, we consider the average “load” of the network

$$\bar{B} = \frac{1}{N} \sum_i B_i = \frac{\sum_i C_i}{2} (N-1) \bar{R}. \quad (31)$$

Similar to Eq. (29), the above expression establishes an exact relationship between the average node betweenness of an arbitrary RW [given by Eq. (25)] and the observables of the associated resistor network, the total edge cost and the average system resistance. For example, for the

$\beta=0$ case, $\bar{B} = \bar{k}N(N-1)\bar{R}/2$. As noted earlier, for calculation purposes one is free to consider the set of C_{ij} coefficients given by Eq. (8), which also leads us to the following statement: *For a RW defined by the transition probabilities Eq. (25), the average RW betweenness is minimal when the average system resistance of the associated resistor network with fixed total edge cost (and the width of the associated noisy synchronization network) is minimal.*

Utilizing again our earlier approximations and results for uncorrelated SF graphs and the relationship between the width and the average system resistance, we find

$$\bar{B}(\beta) = \frac{\sum_i C_i}{2}(N-1)\bar{R} = \left(\sum_i C_i \right) N \langle w^2 \rangle \approx N^2 \frac{(\gamma-1)^2}{(\gamma-2-\beta)(\gamma+\beta)}. \quad (32)$$

The average node betweenness is minimal for $\beta = \beta^* = -1$, for all γ .

4.2 Commute times and hitting times for weighted RWs

The hitting (or first passage) time τ_{st} is the expected number of steps for the random walker originating at node s to reach node t for the first time. Note that using Doyle and Snell's result [84] for the expected number of visits [Eq. (27)], expressed in term of the network propagator [Eq. (28)], one can immediately obtain an expression for the expected first passage time (see Appendix 4). The commute time is the expected number of steps for a "round trip" between nodes s and t , $\tau_{st} + \tau_{ts}$. Relationships between the commute time and the effective two-point resistance have been explored and discussed in detail in several works [85, 130, 131]. In its most general form, applicable to weighted networks, it was shown by Chandra et al. [130] (see also Appendix 4) that

$$\tau_{st} + \tau_{ts} = \left(\sum_i C_i \right) R_{st}. \quad (33)$$

For the average hitting (or first passage) time, averaged over all pairs of nodes, one then obtains

$$\begin{aligned} \bar{\tau} &\equiv \frac{1}{N(N-1)} \sum_{s \neq t} \tau_{s,t} = \frac{1}{2N(N-1)} \sum_{s \neq t} (\tau_{s,t} + \tau_{t,s}) \\ &= \frac{\sum_i C_i}{2N(N-1)} \sum_{s \neq t} R_{st} = \frac{\sum_i C_i}{2} \bar{R}. \end{aligned} \quad (34)$$

Comparing Eq. (31) and (34), the average hitting time (the average travel time for packets to reach their destinations) then can be written as $\bar{\tau} = \bar{B}/(N-1)$. Note that this relationship is just a specific realization of Little's law [136, 137], in the context of general communication networks, stating that the average time needed for a packet to reach its destination is proportional to the total load of the network. Thus, the average hitting time and the average node betweenness (only differing by a factor of $N-1$) are minimized *simultaneously* for the same graph (as a function of β , in our specific problem).

4.3 Network congestion due to queuing limitations

Consider the simplest local "routing" or search problem [67, 70, 72] in which packets are generated at *identical* rate ϕ at each node. Targets for each newly generated packet are chosen uniformly at random from the remaining $N-1$ nodes. Packets perform independent, weighted RWs, using the transition probabilities Eq. (25), until they reach their targets. Further, the

queuing/processing capabilities of the nodes are limited and are identical, e.g. (without loss of generality) each node can send out one packet per unit time. From the above it follows that the network is congestion-free as long as

$$\phi \frac{B_i}{N-1} < 1, \quad (35)$$

for every node i [10, 66, 67, 70, 71, 73]. As the packet creation rate ϕ (network throughput per node) is increased, congestion emerges at a critical value ϕ_c when the inequality in Eq. (35) is first violated. Up to that point, the simple model of independent random walkers (discussed in the previous subsections), can self-consistently describe the average load landscape in the network. Clearly, network throughput is limited by the most congested node (the one with the maximum betweenness), thus

$$\phi_c = \frac{N-1}{B_{\max}}, \quad (36)$$

a standard measure to characterize the efficiency of communication networks [10, 66, 67, 70, 71, 73].

To enhance or optimize network throughput (limited by the onset of congestion at the nodes), one may scale up the processing capabilities of the nodes [70], optimize the underlying network topology [67], or optimize routing by finding pathways which minimize congestion [10, 71–73]. The above RW routing, with the weighting parameter β controlling “hub avoidance”, is an example for the latter, where the task is to maximize global network throughput by locally directing traffic. In general, congestion can also be strongly influenced by “bandwidth” limitations (or collisions of packets), which are related to the edge betweenness, and not considered here.

According to Eq. (36), the network throughput is governed and limited by the largest betweenness in the network. Further, the RW betweenness of the nodes is proportional to the weighted degree, which approximately scales as a power law with the degree in SF networks Eq. (30). Employing the known scaling behavior of the degree cut-off (the scaling of the largest degree) in uncorrelated SF networks [15, 118, 138], one can show that the maximum RW betweenness and network throughput exhibit a minimum and a maximum, respectively, at around $\beta^* \approx -1$ [10]. Here we show numerical results for the RW betweenness and the network throughput in BA SF networks. Figure 4 demonstrates that the RW betweenness is strongly correlated with the degree in SF networks. In particular, except for nodes with very small degrees, $B(k_i) \sim k_i^{\beta+1}$ [Eq. (30)]. For $\beta \approx -1$, the load (RW betweenness) becomes balanced [Fig. 4] and the network throughput exhibits a maximum [Fig. 5]. Thus, RW weights with $\beta \approx -1$ correspond to the optimal hub avoiding weighting scheme.

In a recent, more realistic network traffic simulation study of a congestion-aware routing scheme, Danila et al. [72] found a qualitatively very similar behavior to what we have observed here. In their network traffic simulation model, packets are forwarded to a neighbor with a probability proportional to a power β of the *instantaneous queue length* of the neighbor. They found that there is an optimal value of the exponent β , close to -1 .

We also show numerical results for the network throughput for SW networks with the same degree [Fig. 5(a)]. In particular, an optimally weighted SW network always outperforms its BA scale-free counterpart with the same degree. Qualitatively similar results have been obtained in actual traffic simulation for networks with exponential degree distribution [72].

To summarize, the above simple weighted RW model for local routing on SF networks indicates that the routing scheme is optimal around the value $\beta^* \approx -1$. At this point, the load is balanced [Eq. (30) and Fig. 4(b)], both the average load and the average packet delivery time are minimum, and the network throughput is maximum [Fig. 5].

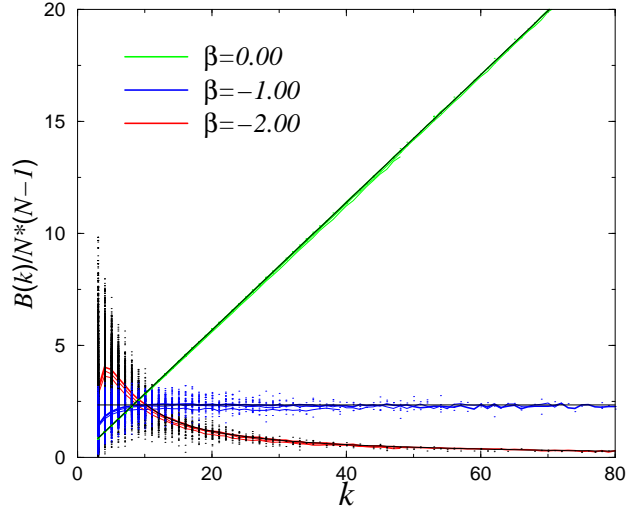


Fig. 4. Normalized RW node betweenness on BA networks with $m=3$ as a function of the degree of the nodes for four system sizes [$N=200$ (dotted), 400 (dashed), 1000 (long-dashed), 2000 (solid)] and for three different β values, $\beta=0.00$, $\beta=-1.00$, and $\beta=-2.00$ (from top to bottom). Data point represented by lines are averaged over all nodes with degree k . Data for different system sizes are essentially indistinguishable. Scatter plot (dots) for the individual nodes is also shown from ten network realizations for $N=1000$. Solid curves, corresponding to the MF+UC scaling $B(k) \sim k^{\beta+1}$ [Eq. (30)], are also shown.

From a viewpoint of network vulnerability [139–143], the above results for the weighted RW routing scheme also implies the following. Network failures are often triggered by large load fluctuations at a specific node, then subsequently cascading through the system [142]. Consider a “normal” operating scenario (i.e., failure is *not* due to intentional/targeted attacks), where one gradually increases the packet creation rate ϕ and the overloaded nodes (ones with the highest betweenness) gradually removed from the network [143]. For $\beta > \beta^* \approx -1$ (including the unweighted RW with $\beta=0$), these nodes are the ones with the highest degrees, but uncorrelated SF networks are structurally vulnerable to removing the hubs. At the optimal value of β , not only the network throughput is maximal, and the average packet delivery time is minimal, but the load is balanced: overloads are essentially equally likely to occur at any node and the underlying SF structure is rather resilient to random node removal [139, 140]. Thus, at the optimal value of β , the local weighted RW routing simultaneously optimizes network performance and makes the network less vulnerable against inherent system failures due to congestions at the processing nodes.

5 Current Flow in Weighted Networks

Current flow in resistor networks provides the simplest distributed flow model in complex networks [92]. This flow is directed and distributed, as the current flows from the highest

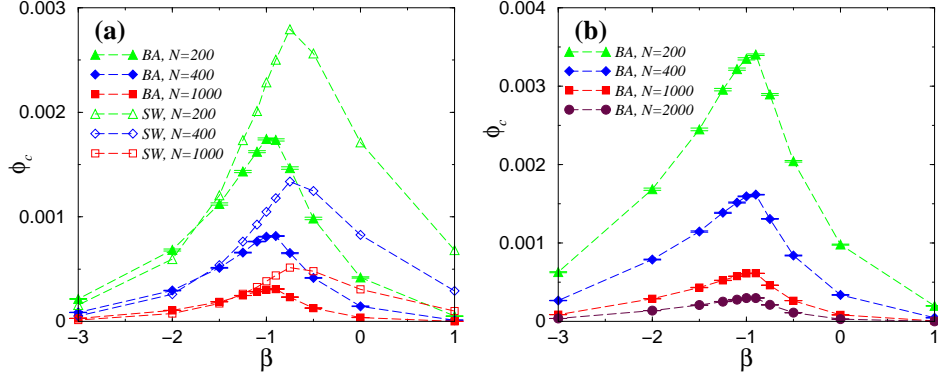


Fig. 5. Network throughput per node as a function of the weighting parameter β for BA networks (solid symbols) for various system size for (a) $m=3$ and for (b) $m=10$ ($\langle k \rangle \simeq 2m$). Figure (a) also shows the same observable for SW networks with the same average degree for the same system sizes (the same respective open symbols).

potential node (source) to the lowest potential node (target). While current can run along all (possibly weighted) paths between the source and target nodes, more current is carried along shorter paths (with smaller resistance). Further, hanging dead ends (i.e., nodes which does not lie on a path between the source and target) will carry zero current. Thus, currents running through the nodes or the links, averaged over all source-target pairs (referred to as the current-flow betweenness), provide a good measure for information centrality, also referred to as current-flow betweenness [126, 127].

Using the same resistor network model as in Sec. 3 where an edge between nodes i and j has conductivity C_{ij} , for a given source (s) and target (t) pair, we can write the potential difference between nodes i and j as

$$V_i - V_j = \hat{V}_i - \hat{V}_j = I(G_{is} - G_{it} - G_{js} + G_{jt}). \quad (37)$$

Here, G_{ij} is the propagator (or pseudo inverse, operating in the space orthogonal to the zero mode) of the network Laplacian. If nodes i and j are connected by an edge in the network, and assuming unit current ($I=1$) entering and leaving the network, then the current through this edge can be expressed as

$$I_{ij}^{st} = C_{ij}(V_i - V_j) = C_{ij}(G_{is} - G_{it} - G_{js} + G_{jt}). \quad (38)$$

Thus, exploiting the conservation of currents, the net current running through node i for a given source-target pair, can be written as

$$I_i^{st} = \frac{1}{2} \sum_j |I_{ij}^{st}| = \frac{1}{2} \sum_j C_{ij} |G_{is} - G_{it} - G_{js} + G_{jt}|. \quad (39)$$

Finally, considering all source-target pairs (where all nodes can simultaneously be sources and send one unit of current per unit time to a randomly chosen target), one finds the current-flow betweenness or information centrality [126, 127],

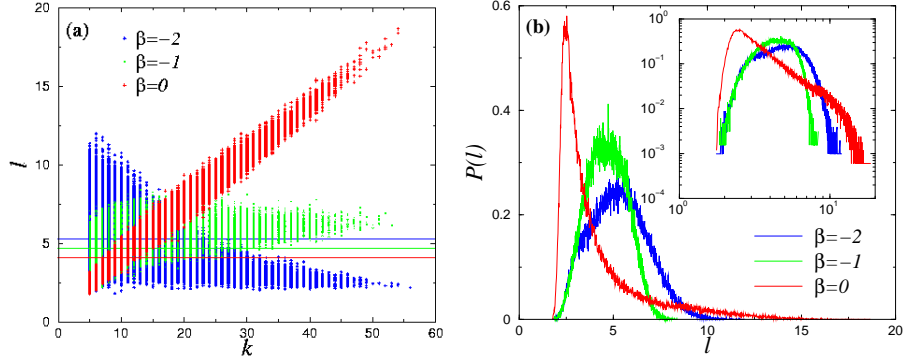


Fig. 6. (a) Scatter plot for the load (current-flow betweenness) vs the degree for BA networks with $N=100$ and $\langle k \rangle \simeq 10$ for three different β values. Horizontal lines indicate the average load. (b) Load distribution of BA networks with the same parameters. The inset shows the same distributions on log-log scales.

$$l_i = \frac{1}{N-1} \sum_{s,t} I_i^{st} = \frac{1}{2(N-1)} \sum_j \sum_{s,t} C_{ij} |G_{is} - G_{it} - G_{js} + G_{jt}|. \quad (40)$$

Despite the similarities between Eqs. (28) and (38), here the summation over source and target pairs does not yield internal cancellations and simplifications, and the result for the current-flow betweenness is not amenable to simple analytic (mean-field-like) approximations. Therefore, we present only numerical results for the resulting current flow betweenness (the local load for unit input currents) l_i . Our numerical scheme was based on the exact numerical diagonalization [144] of the network Laplacian and constructing the pseudo inverse (propagator) G_{ij} using straightforward spectral decomposition. In addition to the local loads at the nodes l_i , and average system load

$$\langle l \rangle = \frac{1}{N} \sum_i l_i = \frac{1}{2N(N-1)} \sum_{i,j} \sum_{s,t} C_{ij} |G_{is} - G_{it} - G_{js} + G_{jt}|, \quad (41)$$

we also measured the largest current flow betweenness $l_{\max} = \max_{i=1,N} \{l_i\}$ in a given network, and then averaged over many network realizations within the same random network ensemble.

We analyzed the above observables for weighted random networks with $C_{ij} \propto (k_j k_i)^\beta$. Figure 6(a) shows that the loads (current-flow betweenness) at the nodes are strongly correlated with their degree in BA scale-free networks for $\beta=0$, while they become much more balanced for $\beta=-1$. Also, for $\beta=0$ (unweighted network) the load distribution exhibits fat tails, while it decays faster than any power law for $\beta=-1$ [Fig. 6(b)]; consequently, the largest load is significantly reduced for $\beta=-1$. This balanced load for $\beta=-1$, however, is achieved at the expense of a somewhat increased average load [Figure 6(a)]. In general, we observe that reducing β leads to an increasing average load [Fig. 7(a)]. Nevertheless, the largest load in a network, potentially triggering cascading load-based failures, exhibits a minimum at around $\beta \approx -1$ [Fig. 7(b)]. In turn, the network throughput, assuming identical source-target rates and unit processing capabilities at each node [analogously to Eq. (36)]

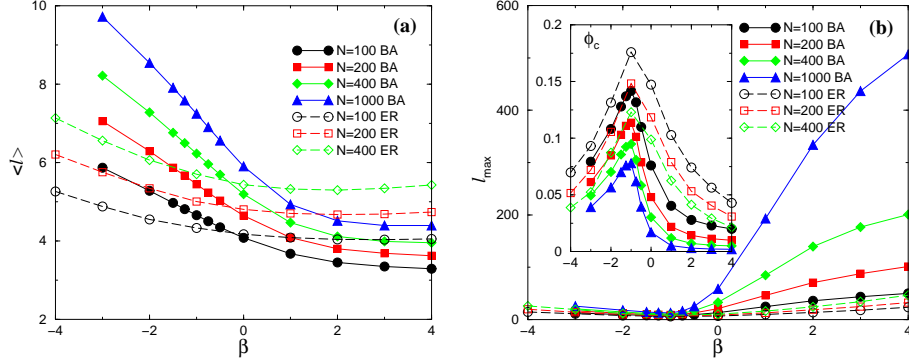


Fig. 7. (a) Average load and (b) maximum load in BA and ER networks with $\langle k \rangle \simeq 10$ for various network sizes as a function of β . The inset in (b) shows the network throughput vs β .

$$\phi_c = \frac{1}{I_{\max}} \quad (42)$$

exhibits a maximum at around $\beta \approx -1$ [Fig. 7(b) inset]. Thus, with the simple weighting scheme $C_{ij} \propto (k_i k_j)^\beta$ one can optimize current flow such that the network throughput is maximum ($\beta^* \approx -1$).

Finally we note that a homogeneous random network [Erdős-Rényi (ER) random graph [14, 145]] exhibits qualitatively similar characteristic in the throughput and load profile as a function of the weighting parameter β [Fig. 7]. Further, as can be seen from Fig. 7(b), the network throughput of an ER network outperforms that of a heterogeneous BA network of the same average degree and network size for any β . Interestingly, the average load is lower for BA (ER) networks for $\beta > 0$ ($\beta < 0$) [Fig. 7(a)].

5.1 Current flow optimization for heterogeneous source/target frequencies

Analogously to the question addressed in Sec 3.1, one can ask what is the optimal weighting of link conductivities to maximize throughput for heterogeneous source/target frequencies. Note that there the task was to maximize global average network conductance with a fixed edge cost. Here, the task is to minimize current-flow betweenness (maximize throughput) subject to identical unit node processing capabilities for a given heterogeneous “boundary condition” (source/target rates). Here, we consider source/target rates proportional to $(k_s k_t)^\rho$, such that the global source/target flow rate per node is ϕ . Then, using Eq. (39), the appropriately weighted current-flow betweenness becomes

$$l_i = \frac{N}{\sum_{s,t} (k_s k_t)^\rho} \sum_{s,t} (k_s k_t)^\rho I_i^{st}. \quad (43)$$

In Fig. 8 we show results for $\rho=1.00$ on BA networks. Similar to homogeneous source/target profiles, the average current-flow betweenness is a monotonically decreasing function of β . The maximum current-flow betweenness $l_{\max} = \max_{i=1,N} \{l_i\}$, however, exhibit a minimum, at around $\beta = -1.50$. In turn, the network throughput $\phi_c = 1/l_{\max}$ shows a maximum at the same point.

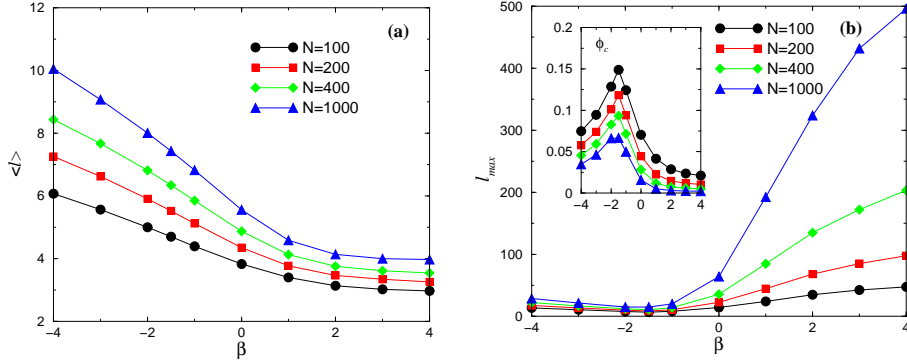


Fig. 8. (a) Average load and (b) maximum load for heterogeneous source/target frequencies with $\rho=1.00$ in BA networks with $\langle k \rangle \simeq 10$ for various network sizes as a function of β . The inset in (b) shows the network throughput vs β .

The behavior of the $\rho=0$ [Fig. 7] and $\rho=1.00$ [Fig. 8] are qualitatively very similar. The main quantitative difference is that the location of the optimal weighting β somewhat decreases ($\beta^* \approx -1.00$ for $\rho=0$ and $\beta^* \approx -1.50$ for $\rho=1.00$). Since the traffic entering and leaving the network places extra burden on the hubs, the negative optimal value of β with a larger magnitude necessitates a relatively stronger hub avoidance.

6 Shortest Path Betweenness in Weighted Networks

In the simplest and most commonly considered models of routing, every source node s sends packets to a given destination node t through the path of least total weight connecting s and t . This path is called the *weighted shortest path* or the *optimal path* between the given source-destination pair. The concept of betweenness previously defined in Sec. 4 can be adapted to the present context as follows: the *shortest path betweenness* of a node (edge) in a weighted network is defined as the number of shortest paths passing through that node (edge) [134]. The characteristics of a variant of the shortest path betweenness defined here - referred to as betweenness centrality - have been studied extensively on unweighted networks (or equivalently, for $\beta = 0$) [52, 53, 146]. Specifically, for scale-free networks with degree exponent $2 \leq \gamma \leq 3$, the distribution of betweenness centrality is known to be heavy tailed, i.e., $P(B) \sim B^{-\delta}$, where δ has been reported to be universal ($\delta \approx 2.2$) [52] or varying slowly [146].

As pointed out in Sec. 4, the throughput of the network (assuming identical unit processing capabilities for each node) is given by $\phi = (N-1)/B_{max}$ where B_{max} is the maximal betweenness of the network [10, 66, 67, 70, 71, 73]. Thus, the throughput can be increased by reducing the maximal betweenness of the network. While the question of a lower bound (optimum) on the scaling of the maximal betweenness B_{max} has been previously studied [71], in the present article we focus on edge weighting schemes that can optimize throughput on the network. We restrict our study to the case where the edge weight connecting to nodes i, j is given by $w_{ij} = (k_i k_j)^{-\beta}$ where k_i, k_j are the degree of nodes i, j respectively. The edge weights considered here can be interpreted as: (1) explicit parameters like latency (time taken to traverse

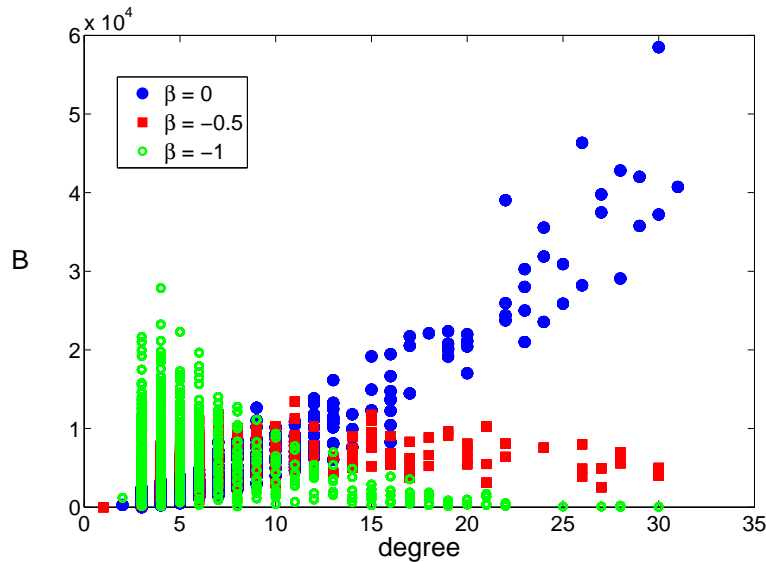


Fig. 9. Scatter plot showing the correlation between degree and betweenness from 10 realizations of weighted scale-free networks with $N=1024$ and degree exponent $\gamma=2.5$ using the configuration model [147]. For an unweighted network $\beta = 0$, betweenness is clearly correlated with the degree. As β is decreased below zero, at $\beta = -0.5$, the betweenness appears to be uncorrelated with the degree, while at $\beta = -1$ betweenness is biased towards lower degree nodes.

an edge) or (2) virtual weights assigned to edges to facilitate the assignment of paths with certain properties like *hub avoidance*. Here, for our numerical investigations, we employed the configuration model [147] with a structural degree cutoff $\sim N^{1/2}$ to generate uncorrelated scale-free graphs [118, 138], with degree exponent $\gamma=2.5$ and with minimum degree $m=2$.

In an unweighted network ($\beta = 0$), the betweenness of a node is known to be correlated with its degree (see Fig. 9). This implies that analogous to the case of random walk routing in Sec. 4, hubs in a scale-free network carry the highest load, and the distribution of betweenness over the network is highly heterogeneous (intuitively, this is obvious since on an unweighted network the shortest path between two nodes is the one with the smallest number of links; since hubs by definition are well connected to the rest of the network, there is some hub that connects the source and destination through a very short path). This can be seen from Fig. 10, where the straight line fit to a logarithmic plot of the betweenness distribution has a slope of ≈ -2.14 . From the point of view of alleviating congestion, and minimizing cascading failures (see Sec. 12), the ideal situation is one where the total betweenness in the network is distributed homogeneously, while keeping the value of the maximal betweenness as low as possible. Homogenizing the betweenness landscape can be achieved by introducing a small amount of hub avoidance as shown by the betweenness distribution for $\beta = -0.5$ in Fig. 10. The tail of the distribution is no longer fat (more appropriately it is exponential, not shown), and the maximal betweenness is lower than for $\beta = 0$ (Fig. 11). Also, betweenness is now no longer correlated with degree (Fig. 9). This homogenization of the betweenness landscape comes at the expense of increasing the average betweenness on the network (see inset, Fig. 10). As β is decreased from -0.5 , rather than further homogenizing the between-

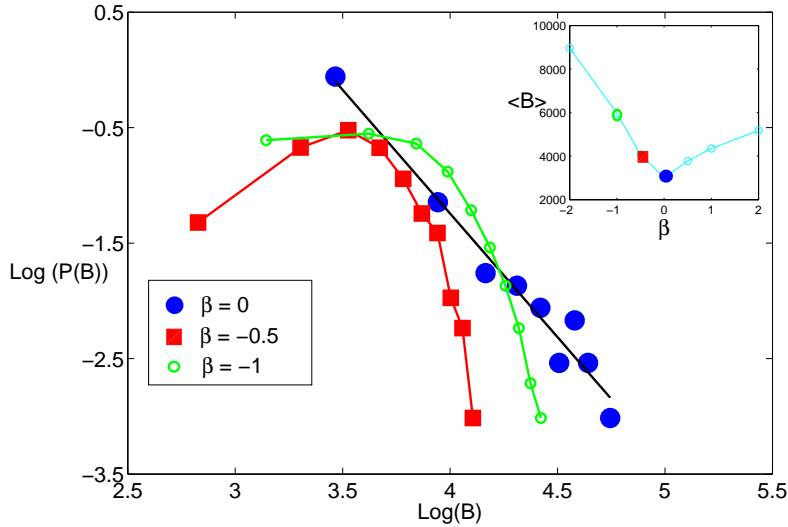


Fig. 10. The distribution of betweenness on weighted scale-free networks with degree exponent $\gamma=2.5$ and network size $N = 1024$. Blue, red and green circles correspond to $\beta = 0, -0.5$ and -1 respectively. The black line is a straight line fit with slope -2.14 . The inset shows the average betweenness $\langle B \rangle$ as a function of β . Results are obtained from 100 network realizations and networks are constructed using the configuration model [147].

ness landscape, the hub avoidance causes the shortest paths to get longer, thus increasing the total betweenness in the network. This increase causes both the average and the maximal betweenness to rise. Furthermore, the betweenness is now largely biased towards nodes of lower degree (Fig. 9). Consequently, the optimal distribution of betweenness is obtained at $\beta = -0.5$ where the throughput is highest. Note that the same observation for the homogenization of the betweenness landscape and the minimization of the maximum betweenness was reported recently by Yang et al. [90] for BA scale free networks ($\gamma=3$). Although there have been some attempts at analytical estimations of the optimal value of β [90], no rigorous arguments are known at present which explain this optimal value. A study of the optimal weight distribution on weighted Erdős-Rényi graphs yields similar results. However, a point worth mentioning is that for similar network size and average degree, the throughput for an Erdős-Rényi network is consistently greater than that of a scale-free network as β is varied (see Fig. 11).

6.1 Cascading Failures and Cascade Control in Weighted Networks

Infrastructure networks with complex interdependencies are known to be vulnerable to *cascading failures*. A cascading failure is a domino effect which originates when the failure of a given node triggers subsequent failures of one or several other nodes, which in turn trigger their own failures. Examples of cascading failures are abundant in the real world, including the "Northeast Blackout of 2003" [148] and the current global economic crisis [149].

The first notable study of cascading failures on networks was by Motter and Lai [150], and the model they proposed is the one we pursue here. The model assumes that in the network

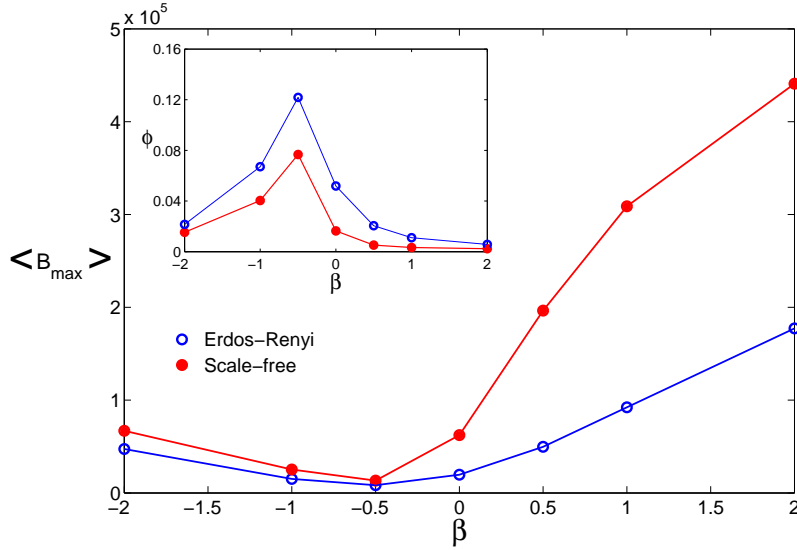


Fig. 11. The average value of the maximal betweenness (over 100 realizations) $\langle B_{max} \rangle$ on weighted scale-free networks and weighted Erdős-Rényi networks of size $N = 1024$. The scale-free networks considered here have degree exponent $\gamma=2.5$ and are constructed using the configuration model [147]. Optimal values of $\langle B_{max} \rangle$ are obtained at $\beta = -0.5$ for both classes of networks.

under consideration each node is transmitting one unit of some quantity (energy, information etc) to every other node through the shortest path between them. As a result, there is some "load" or betweenness incurred on each node which is equal to the number of shortest paths passing through that node. It is assumed that each node is attributed a *capacity* which is the maximum load that can be handled by the node. Since cost constraints prohibit indiscriminately increasing a node's capacity, a natural assumption is that the capacity assigned to a node is proportional to the load that it is expected to handle. Thus [150, 151]

$$C_j = (1 + \alpha)B_j \quad (44)$$

where $\alpha \geq 0$ is a tolerance parameter which quantifies the excess load that a given node can handle. The failure of a node is simulated by the removal of the node and all links connected to it. The functioning of the network after a node failure requires a recomputation of the shortest paths that originally may have passed through the failed node. This redistribution of shortest paths can radically alter the landscape of betweenness on the network. If the redistribution causes certain nodes to have a load greater than their capacity, these nodes also fail. These failures can in turn trigger more failures, thus leading to a cascade. A natural quantity that signifies the severity of a cascade is the ratio of the size of the giant connected component G' remaining after the cascade, to the size of the original giant component, G . Motter and Lai [150] showed that for scale free networks that local failures originating at high degree or high betweenness nodes results in cascades with a high degree of severity. In contrast, a random node failure seldom initiates a cascade, and therefore leaves most of the giant connected component intact.

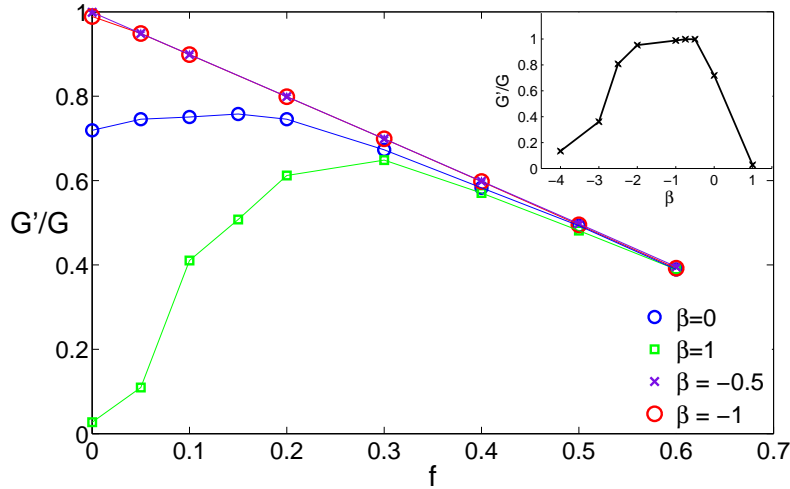


Fig. 12. Simulation results showing the relationship between the fraction of intentionally removed nodes f and the fractional size of the surviving giant connected component G'/G on weighted scale-free networks. Results are for 10 network realizations of scale-free networks with degree exponent $\lambda=2.5$ and $N = 1000$, constructed using the configuration model [147]. The parameter α which quantifies the excess capacity (Eq. 44) is set to 0.5 here. The inset shows the relative size of the giant component of the surviving network vs the weighting parameter β for the $f=0$ baseline scenario (no intentional node removal).

In a subsequent study [152], Motter demonstrated that cascades can be stopped through the intentional removal of nodes after the initial failure has occurred but before the secondary overload failures have begun. One such strategy is to remove a certain fraction f of the nodes with the lowest betweenness. Here we show the results of this procedure extended to weighted networks. In our simulations, cascades are initiated by the removal of the highest betweenness node on a scale-free network with $N=1000$ nodes and with $\alpha = 0.5$. Notice that the damage caused on an unweighted network $\beta = 0$ by a cascade in the absence of any defense strategy ($f = 0$) results in the giant component losing about 30% of its nodes (Fig. 12).

Intentional removals marginally improve the ratio G'/G until a certain optimal value of f beyond which the damage to the network is primarily a result of the intentional removals itself. Thus beyond the optimal f for a given β ,

$$\frac{G'}{G} \approx 1 - f.$$

When β is decreased below zero the shortest paths avoid the hubs, thus alleviating the load on the high degree nodes. For small negative values, $\beta = -0.5, -1$ since the total load on the network is balanced more homogeneously among all the nodes in the network (see Figs. 9 and 10) than on the unweighted network, the size of the cascade dramatically reduces even without any intentional removals i.e. $G'/G \approx 0.99$ at $f = 0$ for both $\beta = -0.5, 1$ (Fig. 12, inset). Furthermore, intentional removals ($f > 0$) only cause further damage. For $\beta = 1$, shortest paths are biased towards the hubs, thereby broadening the fat tail of the load distribution

making it even more heterogeneous than for an unweighted network (not shown). As would be expected, the severity of a cascade in this case is far greater than that in an unweighted network, and consequently the gain arising from intentional removals is also extremely high. At the optimal f , the size of the giant component is greater than half the original network size as opposed to 3% without intentional removals. Thus, in summary for any weighted network there exists an optimal fraction of intentionally removed nodes at which the damage caused by the cascade is the least severe. Furthermore, this optimal removed fraction is very close to zero for a weighted network with $\beta = -1$, thus implying that for this value of β networks are maximally resilient to cascading failures for the network parameters used here.

In the model addressed here, the loads and therefore the capacities result from the particular assignment of shortest paths on the network. Thus the loads and capacities are inherently tied to the topology of the network. An alternative model proposed in [142] looked at similar failure triggered cascades but where the loads on each node were drawn from an arbitrary distribution uncorrelated with the topology of the network. Further studies of cascading failures on weighted networks subject to empirically observed forms of the load-capacity relationship [153] can be found in [89, 90]. The closely related problem of attacking a network by iteratively damaging the node with the highest betweenness and recalculating the betweenness after each damage iteration has been studied in [143, 154].

7 Summary and Outlook

In this Chapter, we considered a simple class of weighted networks in the context of synchronization, flow, and robustness. In particular, we considered weighted edges $C_{ij} \propto A_{ij}(k_i k_j)^\beta$, and investigated optimizing the relevant network observables, i.e., minimizing the width of the synchronization landscape, maximizing the throughput in network flow, or maximizing the size of the surviving giant component following cascading failures (triggered by local overloads).

Our models and methods provided some insights into the challenging problem of optimizing the allocation of limited resources [153, 155] in weighted complex networks. Our results for these fundamental models support that even with this simple one-parameter (β) optimization, one can significantly improve global network performance, as opposed to performing an exhaustive and computationally prohibitive search for optimal weight allocations. It is also important to note that in our optimization problems for RWs (Sec. 4) and flow (Sec. 5 and 6), for simplicity, we considered processing or queuing limitations at the nodes. Within an identical framework, however, one should also consider and study edge-limited flows (motivated by finite bandwidth) with weighted links [156, 157]. Our preliminary results indicate that while optimization is possible, it naturally occurs at a different value of the weighting parameter β . This implies that one cannot optimize and balance traffic for both queueing and bandwidth limitation simultaneously, but instead, trade-offs have to be considered with the knowledge of specific systems.

Real-life information, communication, and infrastructure networks are not only weighted and heterogeneous, but are also spatially embedded [65, 158, 159] and can also exhibit degree correlations [15, 18]. The corresponding metrics (Euclidean distance) strongly influences the cost of the edges, and in turn, the optimal distribution of limited resources. We currently explore and investigate these problems on weighted spatially-embedded complex networks.

Acknowledgement. This research was supported in part by RPI's Seed Grant, NSF Grant No. DMR-0426488, DTRA Award No. HDTRA1-09-1-0049, and by the Army Research Labora-

tory under Cooperative Agreement Number W911NF-09-2-0053. The views and conclusions contained in this document are those of the authors and should not be interpreted as representing the official policies, either expressed or implied, of the Army Research Laboratory or the U.S. Government.

Appendix 1: Globally Optimal Network with Fixed Edge Cost

In this Appendix we determine the the minimum attainable width in the EW synchronization problem for networks with a fixed edge cost. Further, we identify a network which realizes this globally optimal synchronization efficiency. For the EW synchronization problem we can express the total edge cost with the eigenvalues of the network Laplacian,

$$2C_{tot} = \sum_{i,j} C_{ij} = \sum_i C_i = \sum_i \Gamma_{ii} = \text{Tr}(\Gamma) = \sum_{l \neq 0} \lambda_l . \quad (45)$$

Thus, the global optimization problem can be cast as

$$\langle w^2 \rangle = \frac{1}{N} \sum_{l=1}^{N-1} \frac{1}{\lambda_l} = \text{minimum} , \quad (46)$$

with the constraint

$$\sum_{l=1}^{N-1} \lambda_l = 2C_{tot} = \text{fixed} . \quad (47)$$

This elementary extremum problem, Eqs. (46) and (47), immediately yields a solution where all $N-1$ non-zero eigenvalues are equal,

$$\lambda_l = \frac{2C_{tot}}{N-1} , \quad l = 1, 2, \dots, N-1 , \quad (48)$$

and the corresponding *absolute* minimum of the width is

$$\langle w^2 \rangle_{\min} = \frac{(N-1)^2}{2NC_{tot}} . \quad (49)$$

As one can easily see, the above set of identical eigenvalues corresponds to a coupling matrix and network structure where each node is connected to all others with identical strength $C_{ij} = 2C_{tot}/[N(N-1)]$. That is, for fixed cost, the *fully-connected* (FC) network is optimal, yielding the absolute minimum width.

Appendix 2: The Mean-Field Approximation in Stochastic Synchronization on Networks

Summing up the exact equations of motion Eq. (1) over all nodes and exploiting the symmetry $C_{ij} = C_{ji}$ yields the stochastic equation for the mean

$$\partial_t \bar{h} = \xi(t) , \quad (50)$$

where $\xi(t) = \frac{1}{N} \sum_i \eta_i(t)$. From the properties of the individual noise terms in Eq. (1) it follows that $\langle \xi(t) \rangle = 0$ and $\langle \xi(t) \xi(t') \rangle = \frac{2}{N} \delta(t-t')$. Note that the above stochastic equation is exact

for the mean $\bar{h}(t)$. In the mean-field (MF) approximation one replaces the local neighborhood averages by the global mean \bar{h} [Eq. (11)] (which is a crude approximation) yielding

$$\partial_t h_i \approx -C_i (h_i - \bar{h}) + \eta_i(t). \quad (51)$$

Since the time evolution of the mean is now explicit [Eq. (50)], from Eq. (51) we can obtain the approximate equations of motion for the fluctuations with respect to the mean, $\Delta_i(t) \equiv h_i(t) - \bar{h}(t)$,

$$\partial_t \Delta_i(t) \approx -C_i \Delta_i(t) + \tilde{\eta}_i(t), \quad (52)$$

where $\tilde{\eta}_i(t) \equiv \eta_i(t) - \xi(t)$ with $\langle \tilde{\eta}_i(t) \rangle$ and $\langle \tilde{\eta}_i(t) \tilde{\eta}_j(t') \rangle = 2(\delta_{ij} - \frac{1}{N})\delta(t-t')$. From elementary properties of the above linear stochastic differential equations [160] for the equal-time steady-state fluctuations one finds

$$\langle \Delta_i(t) \Delta_j(t) \rangle = \frac{2}{C_i + C_j} (\delta_{ij} - \frac{1}{N}). \quad (53)$$

Thus, the steady-state fluctuations about the mean decouple in the asymptotic large N limit, while $\langle (h_i - \bar{h})^2 \rangle = \langle \Delta_i^2 \rangle \approx 1/C_i$.

Appendix 3: The Weighted Degree for Uncorrelated SF Graphs

Here, we establish an approximate relationship between the weighted degree C_i and the degree k_i of node i for *uncorrelated* (UC) weighted SF graphs. Note that C_i also becomes the effective coupling to the mean in the mean-field approximation of the EW synchronization problem. Using the specific form of the weights as constructed in Eq. (8), we write

$$C_i = \sum_j C_{ij} = N\bar{k} \frac{\sum_j A_{ij} (k_i k_j)^\beta}{\sum_{l,n} A_{ln} (k_l k_n)^\beta} = N\bar{k} \frac{k_i^\beta \sum_j A_{ij} k_j^\beta}{\sum_l k_l^\beta \sum_n A_{ln} k_n^\beta}. \quad (54)$$

For large minimum (and in turn, average) degree, expressions of the form $\sum_j A_{ij} k_j^\beta$ can be approximated as

$$\sum_j A_{ij} k_j^\beta = \left(\sum_j A_{ij} \right) \frac{\sum_j A_{ij} k_j^\beta}{\sum_j A_{ij}} = k_i \frac{\sum_j A_{ij} k_j^\beta}{\sum_j A_{ij}} \approx k_i \int dk P(k|k_i) k^\beta, \quad (55)$$

where $P(k|k')$ is the probability that an edge from node with degree k' connects to a node with degree k . For *uncorrelated* random graphs, $P(k|k')$ does *not* depend on k' , and one has $P(k|k') = kP(k)/\langle k \rangle$ [15, 18], where $P(k)$ is the degree distribution and $\langle k \rangle$ is the ensemble-averaged degree. Thus, Eq. (54), for UC random networks, can be approximated as

$$C_i \approx N\langle k \rangle \frac{k_i^{\beta+1} \int dk P(k|k_i) k^\beta}{N \int dk' k'^{\beta+1} P(k') \int dk P(k|k') k^\beta} = \langle k \rangle \frac{k_i^{\beta+1}}{\int_m^\infty dk' k'^{\beta+1} P(k')}. \quad (56)$$

Here, we consider SF degree distributions,

$$P(k) = (\gamma - 1) m^{\gamma-1} k^{-\gamma}, \quad (57)$$

where m is the minimum degree in the network and $2 < \gamma \leq 3$. The average and the minimum degree are related through $\langle k \rangle = m(\gamma - 1)/(\gamma - 2)$. No upper cutoff is needed for the convergence of the integral in Eq. (56), provided that $2 + \beta - \gamma < 0$, and one finds

$$C_i \approx \frac{\gamma - 2 - \beta}{\gamma - 2} \frac{k_i^{\beta+1}}{m^\beta}. \quad (58)$$

Thus, for uncorrelated random SF graphs with large minimum degree, the effective coupling coefficient C_i only depends on the degree k_i of node i , i.e., for a node with degree k

$$C(k) \approx \frac{\gamma - 2 - \beta}{\gamma - 2} \frac{k^{\beta+1}}{m^\beta}. \quad (59)$$

Appendix 4: RW Hitting Times and the Network Propagator

Employing Doyle and Snell's result [84] for the expected number of visits [Eq. (27)], and expressing the voltage difference of the associated resistor networks in terms of the network propagator (or pseudo inverse of the network Laplacian) [Eq. (19)] one has

$$E_i^{s,t} = C_i(V_i - V_t) = C_i(\hat{V}_i - \hat{V}_t) = C_i(G_{is} - G_{it} - G_{ts} + G_{tt}). \quad (60)$$

Then the hitting (or first passage) time, which is the expected number of steps in a RW which starts at node s and ends upon first reaching node t , can be written as

$$\tau_{st} = \sum_i E_i^{s,t} = \sum_i C_i(G_{is} - G_{it} - G_{ts} + G_{tt}). \quad (61)$$

The expression for the symmetric commute time (expected number of steps for a "round-trip" between nodes s and t) simplifies significantly,

$$\tau_{st} + \tau_{ts} = \sum_i (E_i^{s,t} + E_i^{t,s}) = \sum_i C_i(G_{ss} + G_{tt} - 2G_{ts}) = \left(\sum_i C_i \right) R_{st}, \quad (62)$$

where we used the expression for the two-point resistance of the associated resistor network [Eq. (20)].

References

1. S.H. Strogatz, *Nature* **410**, 268 (2001).
2. S.H. Strogatz, *Synch: the Emerging Science of Spontaneous Order* (Hyperion, New York, 2003).
3. S. Boccaletti, J. Kurths, G. Osipov, D. L. Valladares, and C. S. Zhou, *Phys. Rep.* **366**, 1 (2002).
4. J.A. Acebrón, L.L. Bonilla, C.J. Pérez Vicente, F. Ritort, and R. Spigler, *Rev. Mod. Phys.* **77**, 137 (2005).
5. A. Arenas *et al.*, *Phys. Rep.* **469**, 93 (2008).
6. R. Olfati-Saber, J.A. Fax, and R.M. Murray, *Proc. IEEE* **95**, 215 (2007).
7. R.K. Ahuja, T.L. Magnanti, and J.B. Orlin, *Network Flows: Theory, Algorithms, and Applications* (Prentice Hall, Englewood Cliffs, NJ, 1993).
8. B. Tadic, G.J. Rodgers, and S. Thurner, *Int. J. Bifurcation and Chaos*, **17**, 2363 (2007).
9. L.K. Gallos, C. Song, S. Havlin, and H.A. Makse, *Proc. Natl. Acad. Sci. USA* **104**, 7746 (2007).

10. G. Korniss, Phys. Rev. E **75**, 051121 (2007).
11. A. Schrijver, "Flows in railway optimization", *Nieuw Archief voor Wiskunde* **5/9** 126 (2008).
12. D.J. Watts and S.H. Strogatz, *Nature* **393**, 440 (1998).
13. A.-L. Barabási and R. Albert, *Science* **286**, 509 (1999).
14. R. Albert and A.-L. Barabási, *Rev. Mod. Phys.* **74**, 47 (2002).
15. S.N. Dorogovtsev and J.F.F. Mendes, *Adv. in Phys.* **51**, 1079 (2002).
16. M.E.J. Newman, *SIAM Review* **45**, 167 (2003).
17. L. Li, D. Alderson, R. Tanaka, J.C. Doyle, W. Willinger, *Internet Math.* **2**, 431 (2005); arXiv:cond-mat/0501169.
18. R. Pastor-Satorras and Alessandro Vespignani, *Evolution and Structure of the Internet: A Statistical Physics Approach* (Cambridge University Press, 2004).
19. S. Boccaletti, V. Latora Y. Moreno, M. Chavez, D.-U. Hwang, *Phys. Rep.* **424** 175 (2006).
20. A. Barrat, M. Barthelemy, and Alessandro Vespignani, *Dynamical processes in complex networks* (Cambridge University Press, 2008).
21. G. Korniss, M.A. Novotny, H. Guclu, and Z. Toroczkai, P.A. Rikvold, *Science* **299**, 677 (2003).
22. R. Olfati-Saber and R.M. Murray, *IEEE Trans. Automat. Contr.* **49**, 1520 (2004).
23. R. Olfati-Saber, in *Proc. American Control Conf.* (IEEE, Los Alamitos, CA, 2005), pp. 2371–2378.
24. C.W. Reynolds, *Computer Graphics*, **21**, 25 (1987).
25. T. Vicsek *et al.*, *Phys. Rev. Lett.* **75**, 1226 (1995).
26. F. Cucker and S. Smale, *IEEE Trans. Automat. Contr.* **52**, 852 (2007).
27. J.A. Fax and R.M. Murray, *IEEE Trans. Automat. Contr.* **49**, 1465 (2004).
28. T.I. Netoff, R. Clewley, S. Arno, T. Keck, and J.A. White, *The Journal of Neuroscience* **24**, 8075 (2004).
29. G. Grinstein and R. Linsker, *Proc. Natl. Acad. Sci. USA* **102**, 9948 (2005).
30. E. Izhikevich, *SIAM Rev.* **43**, 315 (2001).
31. Q. Wang, Z. Duan, M. Perc, and G. Chen, *Europhys. Lett.* **83**, 50008 (2008).
32. Q. Wang, M. Perc, Z. Duan, and G. Chen, *Phys. Rev. E* **80**, 026206 (2009).
33. A.T. Winfree, *J. Theor. Biol.* **16**, 15 (1967).
34. D. Lusseau, B. Wilson, P.S. Hammond, K. Grellier, J.W. Durban, K.M. Parsons, T.R. Barton, P.M. Thompson, *Journal of Animal Ecology* **75**, 14 (2006).
35. Y. Rabani, A. Sinclair, and R. Wanka, "Local Divergence of Markov Chains and the Analysis of Iterative Load-Balancing Schemes", in *Proc. 39th Annual Symposium on Foundations of Computer Science* (IEEE Computer Society, Washington, DC, 1998) pp. 694–702.
36. G. Korniss, Z. Toroczkai, M.A. Novotny, and P.A. Rikvold, *Phys. Rev. Lett.* **84**, 1351 (2000).
37. P.M.A. Sloot, B.J. Overeinder, and A. Schoneveld, *Comput. Phys. Commun.* **142**, 76 (2001).
38. S. Kirkpatrick, *Science* **299**, 668 (2003).
39. A. Kolakowska and M. A. Novotny, in *Artificial Intelligence and Computer Science*, edited by S. Shannon (Nova Science Publishers, Inc., New York, 2005), pp. 151–176.
40. A. Schrijver, *Mathematical Programming*, **91**, 437 (2002).
41. A. N. Tolstoi, in *Transportation Planning*, Vol. I, (TransPress of the National Commissariat of Transportation, Moscow, 1930) pp. 23.55.
42. F.L. Hitchcock, *J. of Math. and Phys.* **20**, 224 (1941).

43. L.V. Kantorovich and M.K. Gavurin, in *Collection of Problems of Raising the Efficiency of Transport Performance*, Akademiia Nauk SSSR, Moscow-Leningrad, 1949, pp. 110–138.
44. T.J.C. Koopmans, *Econometrica* **17** (Supplement), 136 (1949).
45. T.E. Harris, F.S. Ross, "Fundamentals of a Method for Evaluating Rail Net Capacities", Research Memorandum RM-1573, The RAND Corporation, Santa Monica, California, 1955.
46. L.R. Ford and D.R. Fulkerson, "Maximal Flow through a Network", Research Memorandum RM-1400, The RAND Corporation, Santa Monica, CA, 1954; *Canadian J. Math.* **8**, 399 (1956).
47. L.R. Ford and D.R. Fulkerson, *Flows in Networks* (Princeton University Press, Princeton, NJ, 1962).
48. D.L. Alderson, *Operations Research* **56**, 1047 (2008).
49. L. Donetti, F. Neri, and M.A. Munoz, *J. Stat. Mech.* P08007 (2006).
50. P. J. Macdonald, E. Almaas, A.-L. Barabási, *Europhys. Lett.* **72**, 308 (2005).
51. A. Barrat, M. Barthélemy, R. Pastor-Satorras, and A. Vespignani, *Proc. Natl. Acad. Sci. USA* **101**, 3747 (2004).
52. K.-I. Goh, B. Kahng, and D. Kim, *Phys. Rev. Lett.* **87**, 278701 (2001).
53. K.-I. Goh, J.D. Noh, B. Kahng, and D. Kim, *Phys. Rev. E* **72**, 017102 (2005).
54. J.D. Noh and H. Rieger, *Phys. Rev. Lett.* **92**, 118701 (2004).
55. L.K. Gallos, *Phys. Rev. E* **70**, 046116 (2004).
56. E. Almaas, R.V. Kulkarni, and D. Stroud, *Phys. Rev. E* **68**, 056105 (2003).
57. M. Argollo de Menezes and A.-L. Barabási, *Phys. Rev. Lett.* **92**, 028701 (2004).
58. E. Almaas, B. Kovacs, T. Vicsek, Z.N. Oltvai and A.-L. Barabási, *Nature* **427**, 839 (2004).
59. Z. Toroczkai and K. Bassler, *Nature* **428**, 716 (2004).
60. R. Guimerà, S. Mossa, A. Turtleschi, and L.A.N. Amaral, *Proc. Natl. Acad. Sci. USA* **102**, 7794 (2005).
61. K. Park, Y.-C. Lai, L. Zhao, and N. Ye, *Phys. Rev. E* **71**, 065105(R) (2005).
62. D.J. Ashton, T.C. Jarrett, and N.F. Johnson, *Phys. Rev. Lett.* **94**, 058701 (2005).
63. D.-S. Lee and H. Rieger, *Europhys. Lett.* **73**, 471 (2006).
64. D. Brockmann, L. Hufnagel, and T. Geisel, *Nature* **439**, 462 (2006).
65. V. Colizza, A. Barrat, M. Barthélemy, and A. Vespignani, *Proc. Natl. Acad. Sci. USA* **103**, 2015 (2006).
66. W. Krause, I. Glauche, R. Sollacher, and M. Greiner, *Physica A* **338**, 633 (2004).
67. R. Guimerà, A. Díaz-Guilera, F. Vega-Redondo, A. Cabrales, and A. Arenas, *Phys. Rev. Lett.* **89**, 248701 (2002).
68. B. Tadić, S. Thurner, G.J. Rodgers, *Phys. Rev. E* **69**, 036102 (2004).
69. P.E. Parris and V.M. Kenkre, *Phys. Rev. E* **72**, 056119 (2005).
70. L. Zhao, Y.-C. Lai, K. Park, and Nong Ye, *Phys. Rev. E* **71**, 026125 (2005).
71. S. Sreenivasan, R. Cohen, E. López, Z. Toroczkai, and H.E. Stanley, *Phys. Rev. E* **75**, 036105 (2007).
72. B. Danila, Y. Yu, S. Earl, J.A. Marsh, Z. Toroczkai, and K.E. Bassler, *Phys. Rev. E* **74**, 046114 (2006).
73. B. Danila, Y. Yu, J.A. Marsh, and K.E. Bassler, *Phys. Rev. E* **74**, 046106 (2006).
74. B. Danila, Y. Yu, J.A. Marsh, and K.E. Bassler, *Chaos* **17**, 026102 (2007).
75. T. Antal and P.L. Krapivsky, *Phys. Rev. E* **74**, 051110 (2006).
76. A. Nagurney and Q. Qiang, *Europhys. Lett.* **79**, 38005 (2007).
77. A. Nagurney and Q. Qiang, *Europhys. Lett.* **80**, 68001 (2007).
78. D.J. Aldous, "Cost-volume relationships for flows through a disordered network", *Math. Oper. Res.* **33**, 769 (2008).

79. J.S. Andrade, Jr., H.J. Herrmann, R.F.S. Andrade, and L.R. da Silva, Phys. Rev. Lett. **94**, 018702 (2005).
80. E. López, S.V. Buldyrev, S. Havlin, and H.E. Stanley, Phys. Rev. Lett. **94**, 248701 (2005).
81. S. Carmi, Z. Wu, E. López, S. Havlin, and H.E. Stanley, Eur. Phys. J. B **57**, 165 (2007).
82. Z. Wu, L.A. Braunstein, S. Havlin, and H.E. Stanley, Phys. Rev. Lett. **96**, 148702 (2006).
83. M. Barthélemy and A. Flammini, J. Stat. Mech. L07002 (2006).
84. P.G. Doyle and J.L. Snell, *Random Walks and Electric Networks*, Carus Mathematical Monograph Series Vol. 22 (The Mathematical Association of America, Washington, DC, 1984), pp. 83–149; arXiv:math.PR/0001057.
85. L. Lovász, *Random Walks on Graphs: A Survey in Combinatorics*, Paul Erdős is Eighty Vol. 2, edited by D. Miklós, V.T. Sós, and T. Szőnyi (János Bolyai Mathematical Society, Budapest, 1996), pp. 353-398; <http://research.microsoft.com/users/lovasz/erdos.ps>.
86. S. Redner, *A Guide to First-Passage Processes* (Cambridge University Press, Cambridge, UK, 2001).
87. G. Korniss, M.B. Hastings, K.E. Bassler, M.J. Berryman, B. Kozma, and D. Abbott, Phys. Lett. A **350**, 324 (2006).
88. C. Zhou, A.E. Motter, and J. Kurths, Phys. Rev. Lett. **96**, 034101 (2006).
89. W.-X. Wang and G. Chen, Phys. Rev. E **77**, 026101 (2008).
90. R. Yang, W.-X. Wang, Y.-C. Lai, and G. Chen, Phys. Rev. E **79**, 026112 (2009).
91. A. Baronchelli and R. Pastor-Satorras, e-print arXiv:0907.3810 (2009).
92. R. Huang, “Flow Optimization in Complex Networks”, M.S. Thesis, Rensselaer Polytechnic Institute, Troy, NY (2010).
93. Y. Kuramoto, in *Proceedings of the International Symposium on Mathematical Problems in Theoretical Physics*, edited by H. Araki, Lecture Notes in Physics Vol. 30 (Springer, New York) p. 420.
94. H. Hong, M.Y. Choi, and B.J. Kim, Phys. Rev. E **65**, 026139 (2002).
95. T. Ichinomiya, Phys. Rev. E **70**, 026116 (2004).
96. D.-S. Lee, Phys. Rev. E **72**, 026208 (2005).
97. M. Barahona and L.M. Pecora, Phys. Rev. Lett. **89**, 054101 (2002).
98. T. Nishikawa, A.E. Motter, Y.-C. Lai, and F.C. Hoppensteadt, Phys. Rev. Lett. **91**, 014101 (2003).
99. A.E. Motter, C. Zhou, and J. Kurths, Europhys. Lett. **69**, 334 (2005).
100. A.E. Motter, C. Zhou, and J. Kurths, Phys. Rev. E. **71**, 016116 (2005).
101. C. Zhou and J. Kurths, Chaos **16**, 015104 (2006).
102. L.M. Pecora and T.L. Carroll, Phys. Rev. Lett **80**, 2109 (1998).
103. S.M. Park and B.J. Kim, Phys. Rev. E **74**, 026114 (2006).
104. T. Nishikawa and A.E. Motter, Phys. Rev. E **73**, 065106(R) (2006).
105. T. Nishikawa and A.E. Motter, Proc. Natl. Acad. Sci. U.S.A. **107**, 10342 (2010).
106. Z. Toroczkai, G. Korniss, M. A. Novotny, and H. Guclu, in *Computational Complexity and Statistical Physics*, edited by A. Percus, G. Istrate, and C. Moore, Santa Fe Institute Studies in the Sciences of Complexity Series (Oxford University Press, 2005), pp. 249–270; arXiv:cond-mat/0304617.
107. H. Guclu, G. Korniss, Z. Toroczkai, arXiv:cond-mat/0701301 (2007).
108. A. Nagurney, J. Cruz, J. Dong, and D. Zhang, European Journal of Operational Research **26**, 120 (2005).
109. S.F. Edwards and D.R. Wilkinson, Proc. R. Soc. London, Ser A **381**, 17 (1982).
110. B. Kozma and G. Korniss, in *Computer Simulation Studies in Condensed Matter Physics XVI*, edited by D.P. Landau, S.P. Lewis, and H.-B. Schüttler, Springer Proceedings in Physics Vol. 95 (Springer-Verlag, Berlin, 2004), pp. 29–33.

111. B. Kozma, M. B. Hastings, and G. Korniss, *Phys. Rev. Lett.* **92**, 108701 (2004).
112. B. Kozma, M. B. Hastings, and G. Korniss, *Phys. Rev. Lett.* **95**, 018701 (2005).
113. B. Kozma, M.B. Hastings, and G. Korniss, in *Noise in Complex Systems and Stochastic Dynamics III*, edited by L.B. Kish, K. Lindenberg, Z. Gingl, Proceedings of SPIE Vol. 5845 (SPIE, Bellingham, WA, 2005) pp.130–138.
114. M. B. Hastings, *Eur. Phys. J. B* **42**, 297 (2004).
115. D. Hunt, G. Korniss, and B.K. Szymanski, *Phys. Rev. Lett.* **105**, 068701 (2010).
116. C. E. La Rocca, L. A. Braunstein, and P. A. Macri, *Phys. Rev. E* **77**, 046120 (2008).
117. C. E. La Rocca, L. A. Braunstein, and P. A. Macri, *Phys. Rev. E* **80**, 026111 (2009).
118. M. Catanzaro, M. Boguña, and R. Pastor-Satorras, *Phys. Rev. E* **71**, 027103 (2005).
119. M.E.J. Newman and D.J. Watts, *Phys. Lett. A* **263**, 341 (1999).
120. R. Monasson, *Eur. Phys. J. B* **12**, 555 (1999).
121. S. Kirkpatrick, *Phys. Rev. Lett.* **27**, 1722 (1971).
122. S. Kirkpatrick, *Rev. Mod. Phys.* **45**, 574 (1973).
123. M.E.J. Newman and M. Girvan, *Phys. Rev. E* **69**, 026113 (2004).
124. F. Wu and B.A. Huberman, *Eur. Phys. J. B.* **38**, 331 (2004).
125. C. Faloutsos, K.S. McCurley, and A. Tomkins, in *Proceedings of the Tenth ACM SIGKDD International Conference on Knowledge Discovery and Data Mining* (ACM Press, New York) pp. 118–127.
126. M.E.J. Newman, *Social Networks* **27**, 39 (2005).
127. U. Brandes and D. Fleischer, *Lecture Notes in Computer Science*, edited by V. Diekert and B. Durand (Springer, NY, 2005) Vol. 3404, pp. 533–544.
128. R. Kaul, Y. Yun, and S.-G. Kim, *Comm. ACM* **52**, 132 (2009).
129. F.Y. Wu, *J. Phys. A* **37**, 6653 (2004).
130. A.K. Chandra, P. Raghavan, W.L. Ruzzo, and R. Smolensky, in *Proceedings of the 21st Annual ACM Symposium on the Theory of Computing* (ACM Press, New York, 1989), pp. 574–586.
131. P. Tetali, *J. Theor. Prob.* **4** 101 (1991).
132. L. Adamic, R.M. Lukose, A.R. Puniyani, and B.A. Huberman, *Phys. Rev. E* **64** 046135 (2001).
133. H.P. Thadakamalla, R. Albert, and S.R.T. Kumara, *Phys. Rev. E* **72** 066128 (2005).
134. L.C. Freeman, *Sociometry* **40**, 35 (1977).
135. L.C. Freeman, *Social Networks* **1**, 215 (1979).
136. J.D.C. Little, *Operations Res.* **9**, 383 (1961).
137. A.O. Allen, *Probability, Statistics, and Queueing Theory with Computer Science Applications*, 2nd ed. (Academic Press, Boston, 1990).
138. M. Boguña, R. Pastor-Satorras, and A. Vespignani, *Eur. Phys. J. B* **38**, 205 (2004).
139. R. Albert, H. Jeong, and A.-L. Barabási, *Nature* **406**, 378 (2000).
140. R. Cohen, K. Erez, D. ben-Avraham, S. Havlin, *Phys. Rev. Lett.* **85**, 4626 (2000).
141. R. Cohen, K. Erez, D. ben-Avraham, S. Havlin, *Phys. Rev. Lett.* **86**, 3682 (2001).
142. Y. Moreno, R. Pastor-Satorras, A. Vázquez, and A. Vespignani, *Europhys. Lett.* **62**, 292 (2006).
143. L. Dall’Asta, A. Barrat, M. Barthélemy, and A. Vespignani, *J. Stat. Mech.* P04006 (2006).
144. W.H. Press, S.A. Teukolsky, W.T. Vetterling, B.P. Flannery *Numerical Recipes in C*, 2nd ed. (Cambridge Univ. Press, Cambridge, 1995), Secs. 11.2 and 11.3.
145. P. Erdős and A. Rényi, *Publ. Math. Inst. Hung. Acad. Sci.* **5**, 17 (1960).
146. M. Barthélemy, *Eur. Phys. J. B* **38**, 1434 (2004).
147. M. Molloy and B. Reed, *Random. Struct. Algorithms* **6**, 161 (1995).

148. http://en.wikipedia.org/wiki/Northeast_blackout_of_2003.
149. Jeffrey Sachs, *Scientific American* **300**, 34 (2009).
150. A.E. Motter and Y.-C. Lai, *Phys. Rev. E* **66**, 065102(R) (2002).
151. L. Zhao, K. Park, and Y.-C. Lai, *Phys. Rev. E* **70**, 035101(R) (2004).
152. A.E. Motter, *Phys. Rev. Lett.* **93**, 098701 (2004).
153. D.-H. Kim and A.E. Motter, *New J. Phys.* **10**, 053022 (2008).
154. P. Holme, B.J. Kim, C.N. Yoon, and S.K. Han, *Phys. Rev. E* **65**, 056109 (2002).
155. D.-H. Kim and A.E. Motter, *J. Phys. A* **41**, 224019 (2008).
156. A. Asztalos, S. Sreenivasan, G. Korniss, and B.K. Szymanski, in preparation.
157. X. Ling, M.-B. Hu, W.-B. Du, R. Jiang, Y.H. Wu, and Q.S. Wu, *Phys. Lett. A* **374**, 4825 (2010).
158. H.P. Thadakamalla, R. Albert, and S.R.T. Kumara, "Search in spatial scale-free networks", *New J. Phys.* **9** 190 (2007).
159. M. Ángeles Serrano, D. Krioukov, and M. Boguñá, "Self-Similarity of Complex Networks and Hidden Metric Spaces", *Phys. Rev. Lett.* **100**, 078701 (2008)
160. C.W. Gardiner, *Handbook of Stochastic Methods* 2nd ed. (Springer-Verlag, New York, 1985).